Schweizerische Eidgenossenschaft
Confédération suisse
Confederazione Svizzera
Confederaziun svizra

Federal Department of the Environment, Transport, Energy and Communications DETEC

Swiss Federal Office of Energy SFOE
Energy Research and Cleantech Division

Final report dated 20.11.2022

SHINE: Swiss Hybrid INvErter

Hybrid PE Inverter for Automotive Vehicles

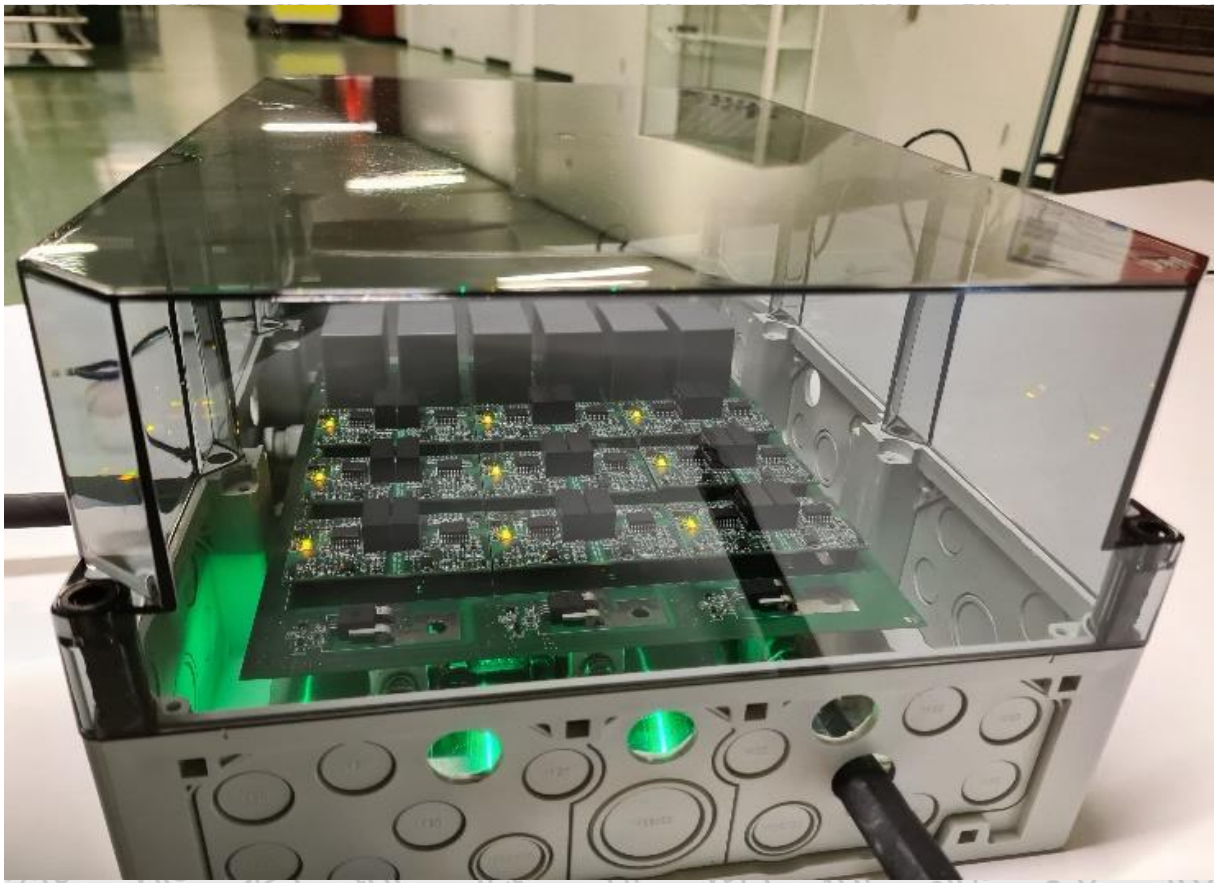

Source: Institute für elektrische Energie Technik, HT FHNW

Date: 20. November 2022

Location: Bern

Publisher:
Swiss Federal Office of Energy SFOE
Energy Research and Cleantech
CH-3003 Bern
www.bfe.admin.ch

Co-financing:
MTAL GmbH
Unterer Schafmattweg 39A
Gänsbrunnen SO
CH-4716

Subsidy recipients:
Prof. Dr. Silvia Mastellone
FHNW Fachhochschule Nordwestschweiz
Klosterzelgstrasse 2
5210, Windisch
www.fhnw.ch

Authors:
Prof. Dr. Silvia Mastellone, FHNW, silvia.matellone@fhnw.ch
Prof. Dr. Renato Minamisawa, FHNW, renato.minamisawa@fhnw.ch

SFOE project coordinators:
SFOE head of domain: Dr Michael Moser, michael.moser@bfe.admin.ch
SFOE programme manager: Roland Brüniger, roland.brueniger@brueniger.swiss

SFOE contract number: SI/501784-01

Zusammenfassung

Im Rahmen des Projekts SHINE haben wir eine neue Leistungselektronik-Topologie namens Adjustable Hybrid Switching (AHS) für Anwendungen im Bereich der Elektromobilität entwickelt und ihr Potenzial unter verschiedenen Konfigurationen und Antriebsprofilen bewertet. Der AHS-Wechselrichter besteht aus XS-Cross-Hybrid-Bauelementen, die aus parallelen SiC- und Si-Bauelementen zusammengesetzt sind, die je nach Laststrombedarf geschaltet werden und wie ein "elektrisches Getriebe" für den Stromrichter arbeiten.

Zunächst wurde ein dynamischer Schalttester gebaut, um die Schaltverluste der Hybridschalter mit verschiedenen Verhältnissen von Si-IGBTs zu SiC-MOSFETs zu ermitteln. Dies war notwendig, da keine Daten über die Verluste in Parallelschaltern verfügbar sind. Diese Verluste wurden als Input für Simulationen verwendet, um systematisch die Leistungseffizienz für verschiedene WLTP-Fahrzyklen zu extrahieren und die optimalen Wechselrichterkonfigurationen zu definieren.

Die optimale AHS-Konfiguration, die aus der Analyse des Kosten-Nutzen-Verhältnisses ermittelt wurde, ist ein Verhältnis von 1:4 SiC-MOSFETs zu Si-IGBTs. Die Simulationsergebnisse zeigen, dass Voll-SiC-Wechselrichter im Vergleich zu Voll-Si-Wechselrichtern eine Effizienzsteigerung von bis zu 9 % aufweisen, basierend auf typischen WLTP-Zyklen. Im Vergleich dazu zeigte der AHS eine Verbesserung des Wirkungsgrads zwischen 5 und 8 % gegenüber dem vollständigen Si-Wandler, während er auf Halbleiterebene 2,5 Mal billiger ist. Der AHS zeigte auch eine Effizienzverbesserung gegenüber dem XS-Hybrid. Aufgrund der unabhängigen Gate-Drive-Steuerung bietet die AHS-Topologie im Vergleich zu ihren Si- und SiC-Pendants eine überlegene Redundanz im Falle eines Ausfalls der individuellen Gate-Steuerung.

Summary

In the project SHINE, we have developed a new power electronics topology called Adjustable Hybrid Switching (AHS) for electric mobility applications, and have evaluated its potential under different configurations and drive profiles. The AHS inverter consists of XS-cross hybrid devices composed from parallel SiC and Si devices, which are switched based on load current demand, working like an “electric gear” for the power converter.

First, a dynamic switching tester has been built to extract the switching losses of the hybrid switches with different ratios of Si-IGBTs to SiC-MOSFETs. This was necessary because there is no data available for losses in parallel switches. Such losses were used as input for simulations in order systematically extract the power efficiency for different WLTP drive cycles and to define the optimum inverter configurations.

The optimum AHS configuration determined from the cost-efficiency trade-off analysis was found to be the ration of 1:4 SiC MOSFET to Si IGBTs. Simulation results show that full SiC inverters exhibit up to 9% efficiency enhancement compared to full Si inverter, based on typical WLTP cycles. Comparably, the AHS demonstrated improvement between 5% and 8% efficiency over the full Si converter consistently, while being 2.5 times cheaper at semiconductor level. The AHS also exhibited efficiency improvement over the XS-hybrid. Because of the independent gate drive control, the AHS topology offers superior redundancy compared to its Si, and SiC counterparts in case of individual gate control failure.

Take-home Messages

The AHS has high potential for electrical vehicle applications over a wide power range, providing a balanced trade-off between the high efficiency of the SiC inverter and the reduced cost of Si counterpart. Because the control optimization profits from the use of SiC devices at sub-load and Si devices at full power load regimes, it has the potential to benefit any variable frequency drive application. However, it benefits are highly dependent on the load profile and device ratio configuration, which needs to be matched for maximum advantage. Further, it is important to keep in mind that full SiC inverters will always be the preferred solution for applications without cost constraints and that require small footprint. In automotive, that could be the case for the lower grade EV segment.

Other application could be in MV traction, MV industrial motors, LV motors, EV chargers, battery inverters and PV inverters. Just to have an idea, in the late example, the AHS could profit PV inverters because this particular market is price sensitive, has no size constraints, and the financial gain with saving in electricity costs is massive. In this case, the AHS would offer the perfect efficiency-cost trade-off. Our next research steps will focus in this direction.

Contents

Abbreviations

AC	Alternating Current
AHS	Adjustable Hybrid Switch
CAD	Computer Aided Design
DAQ	Data Acquisition
DC	Direct Current
DPT	Double Pulse Test
DUT	Device Under Test
E-Car	Electric Cars
EV	Electric Vehicle
FHNW	Fachhochschule Nordwestschweiz
HV	High Voltage
IC	Internal Combustion
IM	Induction Motor
PCB	Printed Circuit Board
PMSM	Permanent Magnet Synchronous Machine
PWM	Pulse Width Modulation
RL	Resistive-Inductive
RC-IGBT	Reverse Conducting Insulated Gate Bipolar Transistor
SFOE	Swiss Federal Office of Energy
SiC	Silicon Carbide
SiC MOSFET	Silicon Carbide Metal Oxide Semiconductor Field Effect Transistor
Si IGBT	Silicon Insulated Gate Bipolar Transistor
SMD	Surface Mounted Device
SOA	Safe Operating Area
SPST	Single Pole Single Throw
VSI	Voltage Source Inverter
WBG	Wide Band Gap
WLTC	Worldwide Harmonized Light Vehicles Test Cycles

1 Introduction

1.1 Background information and current situation

Electric vehicles are gaining popularity nowadays and is on the path for the complete replacement of the IC engine vehicles to reduce or replace fossil fuel and reduce CO2 emission. However, the choice between an IC engine or E-car develops confusion among consumers regarding the maximum distance range that an E-car can travel on a single charge. This is not only dependent on the energy efficiency of the batteries in EV, but also on the overall efficiency of system consisting of mainly batteries, the inverter, and the rotating machine. The inverter is the power electronic component responsible for converting the direct current to alternating current and adds to the losses that can limit the range of an electric vehicle. Thus, improving the efficiency of inverter is a must for the better adaption of EV's in present day market.

Currently, there are no standards for power electronics in EV in terms of system level like packaging, topology, and control. Currently, every major automotive manufacturer (e.g., Toyota, Mitsubishi, Ford, Renault, Nissan) is considering different converter concepts and developing individual platforms. Si IGBTs are seen as the main switching element in a power electronic converter. However, this era is undergoing significant changes with the application of wide band-gap semiconductor devices, such as SiC or GaN MOSFETs, according to their increased high switching speed, junction operation temperature, low thermal resistance, etc. Prototype inverter systems equipped with SiC-MOSFETs demonstrated a marked loss reduction compared with that of a conventional inverter system with Si power devices. With the use of SiC MOSFET, the switching frequency of the converter for same power rating can be increased by around 10 times as compared to Si IGBT or Si BiMOSFET. This certainly can reduce the overall system cost by reducing the size of the passive elements.

However, the cost of individual SiC devices are very high compared to Si IGBT resulting in additional losses. The extremely high cost of substrate and epitaxial material along with the high conduction losses under high voltage and high temperature is a major problem for widespread adoption of SiC power devices. Another disadvantage of those devices is the poor fault current against short circuit events. SiC devices and modules have reported as difficult to parallelize due to gate control instabilities, resulting in failures. Si IGBTs, in turn, are cheap, offer enhanced fault protection and are available in different current ratings and packages. Finally, another challenge for SiC devices is the constant development of Si IGBT (or RC-IGBTs), which are constantly improving in terms of performance, SOA, high temperature operation and reliability, becoming very cost-effective.

A solution providing the benefits of both technologies while addressing the efficiency, and cost effectiveness will enable the automotive industry to move towards the adoption of EV on a large scale. The combination of bipolar Si IGBT and unipolar SiC MOSFET referred to as the cross-switch (XS) hybrid aims to reach optimum power device performance by providing low static and dynamic losses along with improving the overall electrical and thermal properties. This facilitates the soft switching of the slow Si IGBT and enables the hybrid switch as a high frequency switch. The parallel operation of these devices, compared to a standalone Si IGBT, should produce a better switching performance due to the presence of a WBG device [1].

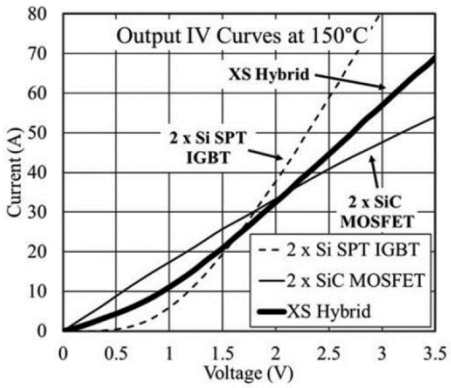

Figure 1. Output characteristics of Hybrid switches

Figure 1 shows the conduction IV curves for the SiC MOSFET in comparison with Si IGBTs and the XS-Hybrid. Be-low the cross-point of about 1.7V the SiC MOSFET offers higher current than the Si IGBT, which inverts at higher voltages [1]. Therefore, for applications where low voltage and high voltage occur, the XS-Hybrid offers lower conduction losses over the full current range. This is the case for transport applications, where the speed and torque of the engine varies, thus requiring low and high current frequently. As such, the SiC MOSFET will take the partial load and the Si IGBT will handle most of inrush loads. Therefore, partial operation of transistors in XS-Hybrid switch based on load is an addable feature to ensure lower switching losses which otherwise is persistent in all load profiles irrespective of the type of the transistor.

This work presents a converter for electric vehicle application with the hybrid switch as its main power switching element. Instead of the conventional hybrid switch configuration of 1:1 SiC to Si, hybrid switch with a different ratio of SiC to Si is investigated here. Simulation of a three-phase inverter, experimental dynamic characterization, cost analysis are some of the primary investigations conducted. In this work, we also introduce the concept of electronic gears wherein switch ratio is adjusted within the range of selected ratio depending on the load condition. A prototype of the proposed concept for the EV application is demonstrated and experimentally characterized.

The greatest advantage of the concept is the significantly lower cost with respect to the full SiC solution combined with higher energy efficiency compared to both full Si/SiC solutions depending on the load condition.

1.2 Purpose of the project

The goal of the SHINE project is to develop a geared three-phase inverter for electric vehicle application based on XS-Hybrid switch. The concept aims to develop a powerful, efficient, and reliable converter while maintaining low cost, size, weight, and parasitic effects. A better efficiency than the full Si IGBT based solution and lower cost than the SiC MOSFET solution is expected in the three phase XS-Hybrid inverter. The gearing system ensures that a transistor is switched on or off according to the situation in which the vehicle is in like acceleration, deceleration, constant velocity, or braking. Thus, the geared cross hybrid inverter is a controller that can adopt different power ratings depending on the load (torque and speed of the car). This provides the benefit that not all the transistors are in working conditions always and improves the overall life span of the power electronics by reducing the probabilities of IGBT or MOSFET failures.

1.3 Objectives

To achieve the goal of the SHINE, the following objectives have been defined:

- Characterization of the XS-Hybrid device
- Designing, constructing, and characterizing the hybrid inverter at TRL5 stage (prototype demonstration in a relevant environment)
- Development of a modular reconfigurable simulation environment and efficiency analysis
- Optimal layout and operation (e-gear)

2 Procedures and methodology

The following procedures have been followed for the realization of each respective goal:

Devices Characterization

Double pulse tester: we characterized the conduction and switching losses of the commercial Si IGBT and SiC MOSFET devices for the simulation calibration. Within these activities, we designed and built a customized double pulse tester.
The tester can characterize different types and ratios of 1.2 kV Si and SiC discrete devices up to a total current of 500A. Both reverse conducting and co-pack Silicon IGBTs in combination with SiC MOSFETs are subjected to test. The results supported the selection of the type of semiconductor and the ratio of SiC to Si devices in hybrid configuration. The double-pulse test is also used to extract switching losses of the hybrid switches that are then used to calibrate the simulations.

Mixed mode simulation: we developed simulation platforms to design and test the XS-Cross-hybrid switch. Mixed mode simulations allow the realistic characterization of the inverter performance while providing information of specific device losses, failure mechanisms and device temperature that cannot be easily achieved experimentally.

Reliability test for the semiconductor devices:
Through H3TRB reliability test we have qualified power semiconductors that then used in the development of the inverter prototype. Further, we built a power/temperature cycling tester to extract reliability model parameters to be using for the diagnostics and prognostics.

Converter Prototype

Development of designs for a three phase XS-Hybrid geared inverter for electric vehicle applications.
This includes the design of the different stages of the three phase XS-Hybrid geared EV inverter. The test environment for an EV drivetrain was restricted to 25 kW and hence the rating of the miniaturized electric inverter prototype. Finally, the hardware prototype has been tested in a laboratory environment to determine its efficiency under a variety of loads calibrated to torque profile of a real vehicle. Later, an experimental platform comprising an EV drivetrain was created in the laboratory. This platform can imitate real life driving situations and tests the compatibility of the inverter with an EV motor and an electric brake.

Simulation platform and efficiency analysis

We developed a modular configurable simulation platform to support efficiency analysis and XS-Hybrid inverter layout configuration. This includes three modules: the first module models the power train and can be reconfigured to cover different car models of various power range driving under different conditions. A second module was developed to define the car mission profile in terms of shaft torque and speed required to follow a specific drive cycle.

A third simulation module was developed to compute the converter losses that are associated to a specific car and mission profile for the three different converter models: Si-, SiC- and hybrid-based converters.

Efficiency Analysis: Based on the developed model simulation, a set of tests have been performed under different testing conditions to compare the performance of Si, SiC and hybrid- based converters in terms of power losses.

Optimal layout and Control Design

The complete modular configurable simulation platform including efficiency models has been employed to define the optimal configuration for each vehicle class.

An optimization routine has been developed to define, for each vehicle class, the optimal XS-Hybrid combination and device brands to maximize efficiency at a minimum cost.

The efficiency-cost analysis for the XS-Hybrid converter evaluates the efficiency of each converter configuration based on device losses and cost, considering different ratios of Si and SiC devices and different brands. An efficiency-cost score has been defined as an index to classify the best layout for each car class.

Finally, an electric gear controller has been designed to optimize the torque and the active semiconductor ratio based on efficiency, and performance requirements.

3 Results and discussion

3.1 Summary Results Device Characterization

Double pulse test system

Because current is shared in hybrid switches between the SiC MOSFET and the Si IGBT, simulations fail to provide accurate values for switching losses. As such, we have designed and constructed a double pulse test rated at 1200 V and 500 A able to characterize different combinations of the hybrid switch configuration. The first set of tests were conducted on the 1.2 kV, 20 A rated SiC MOSFETs from Cree and RC-IGBTs from Infineon. In the second run of tests, RC IGBTs was replaced by 15 A rated IGBTs in co-packs.

Figure 2 illustrates a double pulse circuit diagram, that consists of half bridge configuration with device under test in the lower position. An inductive load is placed in parallel with a free-wheeling diode in the upper switch position. It can be a diode or the same device as the DUT in off mode. This testing configuration is useful for studying switching-energy characteristics of the DUT. The waveforms of interest are gate-source voltage, drain-source voltage, and drain current.

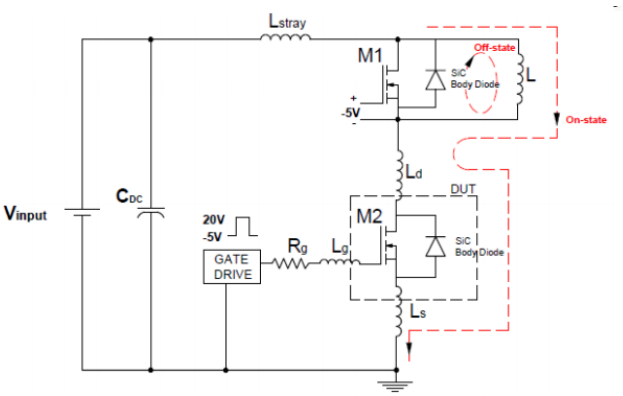

Figure 2. Double pulse tester circuit diagram showing the freewheeling diode on top and the DUT in the bottom.

The double-pulse test is used to measure the switching transients of a device under test (DUT, here hybrid switch). In the test, two gate signals are applied back-to-back to the gate terminal of the device under test with respect to the source terminal. This is the reason why this circuit is more commonly known as the double pulse tester (DPT) circuit. The double-pulse test is normally done with a purely inductive load, i.e., a load inductor. The first pulse (T_1) should turn on the transistor and charge a current through the inductor. This means that the first pulse should be a wide pulse, which charges the load current to the magnitude that is interesting to analyze. Then, in short break interval (T_{break}), the semiconductor is forcefully turned off and the freewheeling diode takes over the residual current of inductor. The time difference between the first and the second pulse is desirably small enough to not let the inductor current fall below the desired level, however, wide enough to allow the turnoff of the device. This is followed by a second short pulse (T_2) where the transistor is turned on again.

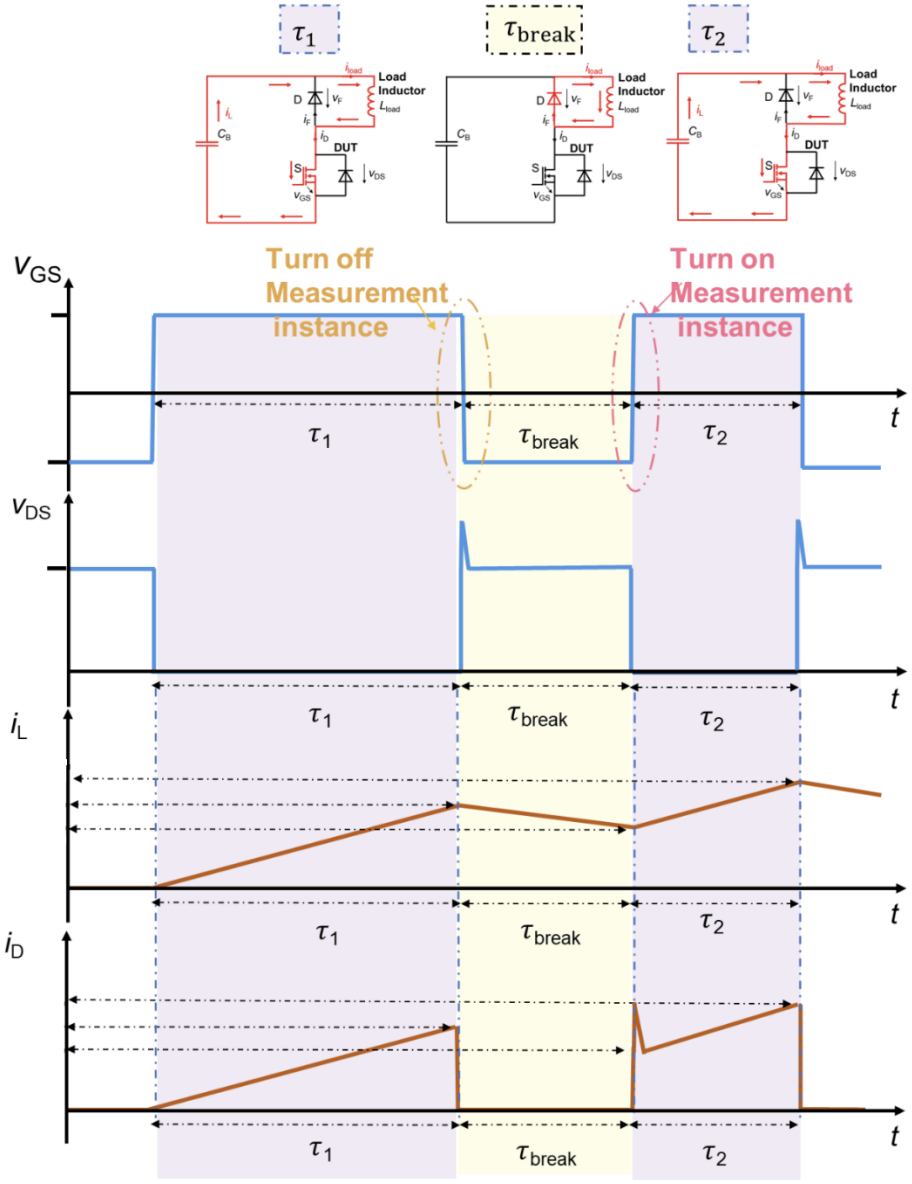

Figure 3. Double pulse signal used to test power semiconductors.

Such a double pulse gives the possibility of analyzing the rising edge (turn on) and the falling edge (turn off) of a hard-switching transient of the transistor at the exact transistor current that is desired. The turn-on and turn-off losses during the switching of the device can be obtained by integrating the voltage and current across the device channel in the respective region. A double-pulse signal and current flow in the double pulse test circuit is depicted in Figure 3.

The double pulses are supplied at a very low frequency, e.g., 1 Hz. This gives the transistor time to remove the generated heat, and the load inductor time to discharge between the double pulses. The first pulse width, in conjunction with the inductor value and bus voltage, determines the current amplitude through the device during the turn-off event. This allows the same set of operating parameters to be applied to the device during the rising edge of the second pulse, the turn-on event.

The DC link capacitance is sized so that it can maintain the desired bus voltage throughout the test after being disconnected from the DC power supply. This improves measurement conditions by minimizing the risk of ringing during transient events caused by ground loops. Such strategic placement of these capacitors helps to cancel the effect of the parasitic inductance from the DC bus connections and from the bulk capacitor to the switching cell. This helps to eliminate the switching ringing and the resulting overshoots on the voltage across the device.

Figure 4 shows the double pulse tester customized for XS-Hybrid switches, featuring the power supply, inductors, bus-bar, protection and the customized DUT PCB.

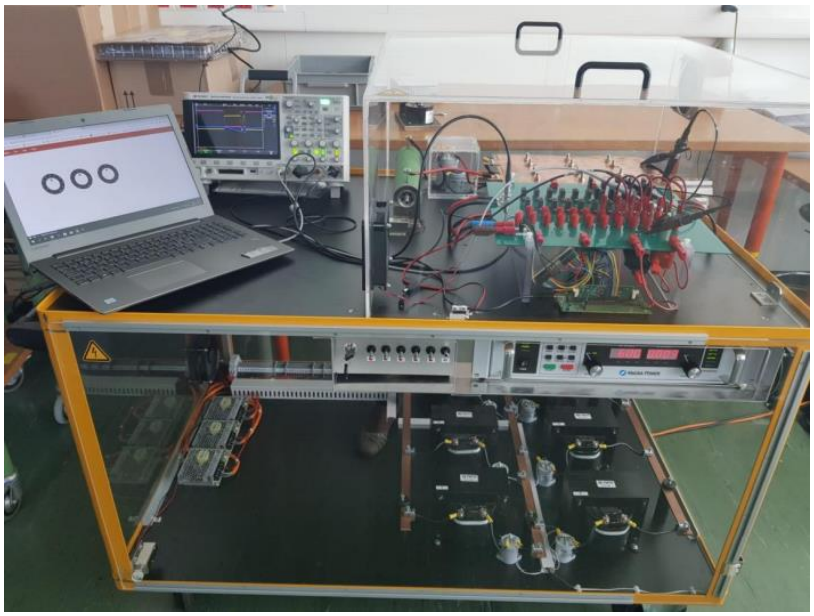

Figure 4. Picture of the XS-cross hybrid double pulse tester.

Stray inductance is the main factor causing dc bus overshoots and voltage spikes across semiconductor switching devices, which is particularly critical for fast switching devices such as SiC MOSFETs. To limit switching losses, the allowed switching frequency must be decreased. Furthermore, significant parasitic high-frequency oscillations appear whenever the loop inductance between dc link capacitors, bus bars and power devices become large. The high values produced during commutations by these fast-switching devices and diodes are currently the main source of conducted and radiated noise emissions because the parasitic layout inductance cannot be fully eliminated. The simplest method to limit undesired high-dynamic overvoltage is the reduction of the distributed inductances throughout the converter and its components. The traditional methods of power distribution inside the power converter (using cable) are no longer compatible with the new packaging and high-speed switching technology. Using a busbar can mitigate this problem by providing lower stray inductance and lower characteristic impedance. Consequently, a greater noise attenuation can be realized. It is known that the planar type of bus bar is best suited for these applications and hence we implement such a design in our tester. This is composed by two parallel conducting plates of resistivity, separated by a dielectric material with relative permittivity, relative permeability, and dielectric conductivity. The two terminals of each of the six capacitors designed in the previous section is connected to the positive and negative plates of the bus bar. This connects all the capacitors in parallel and forms the DC link with values of 300uF or 560uF. The dimensions of the capacitors are taken from the datasheets and are computer drawn using the CAD software. Holes are drawn for the screws of the Capacitors and extra allowance is provided based on the electrical clearance norms. For a voltage of 1700V, clearance of 8.5 mm is provided on the terminal

points where +/-screws meet the opposite charged plates. A planar area covering all the capacitors are selected and hence the dimensions of the plates are: 350 X 250 mm. Two Copper plates with a thickness of 1mm and mentioned dimension is used as the plates.

Six inductors are connected in parallel to supply the load across the upper device. This guarantees that one can vary the load inductance based on the current and in turn the number of devices used for the test. The inductors are connected in parallel with its one terminal connected to a common positive metal plate via high voltage dc relays and other terminal to the negative plate. The relays with the control voltage of 12 V are powered through one of the auxiliary supplies and SPST led switches laid on a control board. Thus, turning on or off the switches on the control board can activate the required inductor.

The double pulse is applied to the DUTs at very low frequency, typically at 1Hz. This ensures that the devices are not overheated. However, this tester is rated at 500A, and hence proper cooling system must be ensured as additional safety. A mechanical protection housing is mounted with exhaust fans to supply proper ventilation through the inner system. In addition, all the separate DUTs and its corresponding reverse biased device are cooled with the help of the individual heat sinks (not shown).

The power PCB holds the sockets for DUTs, the banana sockets for gate drives, sockets for desat connections, lug plates for connection of external cables, probe hooks, pins for auxiliary supply to gate drivers, current shunt and SMD capacitors. The final PCB with all the soldering done is shown in Figure 5. The system allows to measure up to 10 discrete devices in parallel, allowing the different combination of SiC MOSFETs and Si IGBTs. In this project, we customized the PCB for the characterization of H3TRB reliability qualified TO-247 packaged devices. The 10 devices of same as DUTs are used as freewheeling diodes while the ones in the bottom are the real DUTs. The SiC MOSFET channel is used as the freewheeling diode, while the RC-IGBT is operated in PiN diode mode under reverse bias.

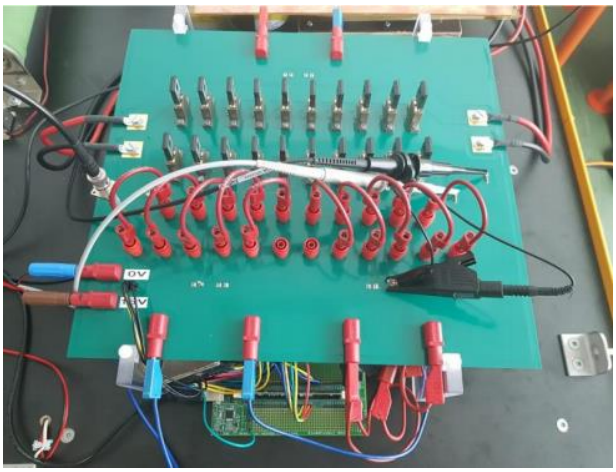

Figure 5. Power PCB for the XS-cross hybrid double pulse tester.

Figure 6 displays the switching waveforms for a XS-hybrid switch featuring SiC MOSFETs and Si RC-IGBTs, showing the turn-on and turn-off events.

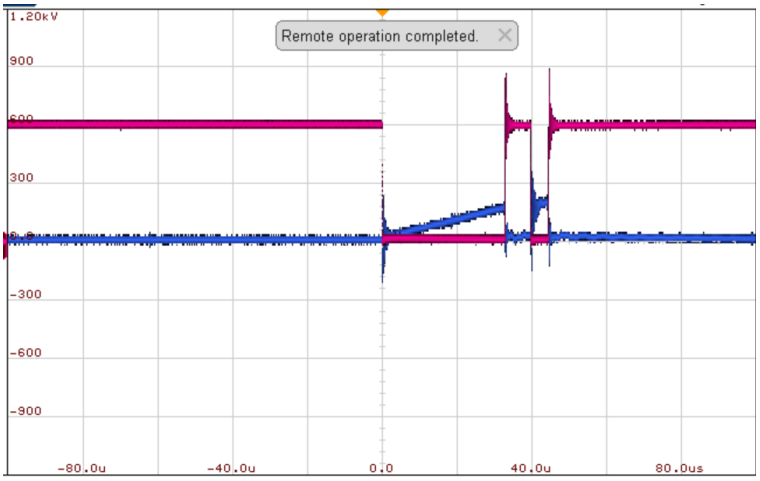

Figure 6. Typical switching waveforms for the XS-cross hybrid switches.

Figure 7 shows the total switching losses (turn-on + turn-off) versus the number of SiC MOSFETs measured from 10 devices in parallel. As shown, the full IGBT combination features up to three times more losses than the full SiC combination. The switching losses of individual SiC MOSFETs or Si IGBTs have been characterized in the system, exhibiting comparable values to those reported in the datasheet.

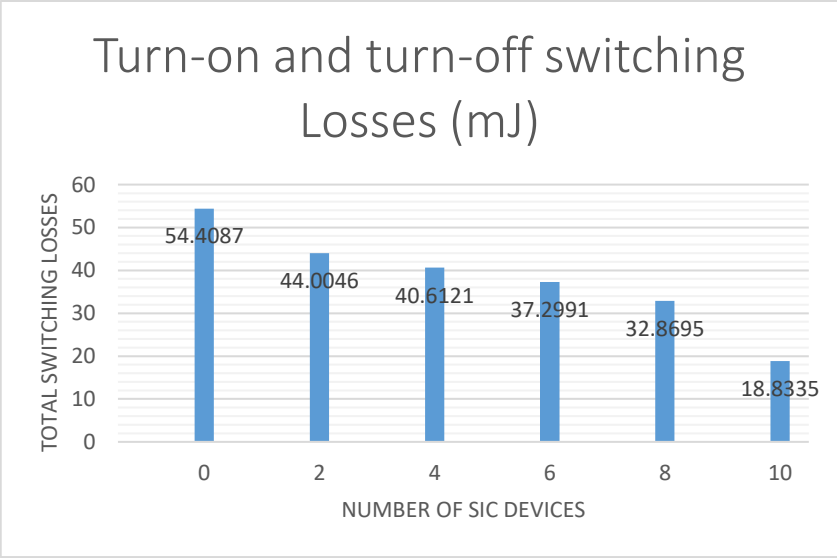

Figure 7. Total switching losses of different combinations of SiC MOSFETs and Si RC-IGBTs.

The experimental procedure was repeated on 15 A rated co-pack IGBTs from Infineon after the short circuit failures of the reverse conducting IGBTs at higher voltages. The PCB of the existing double pulse tester was replaced with a new one to avoid the problem of parasitic inductances. This new PCB was in a similar design to the inverter PCB design and hence gives closer results to the real application. Therefore, the PCB could only measure a maximum of up to 5 devices in parallel. Coaxial shunts were no longer used and high bandwidth hall effect sensors were used in place. Instead of sockets, the semiconductors are always soldered and desoldered from the PCB. The experimental setup is shown in Figure 8.

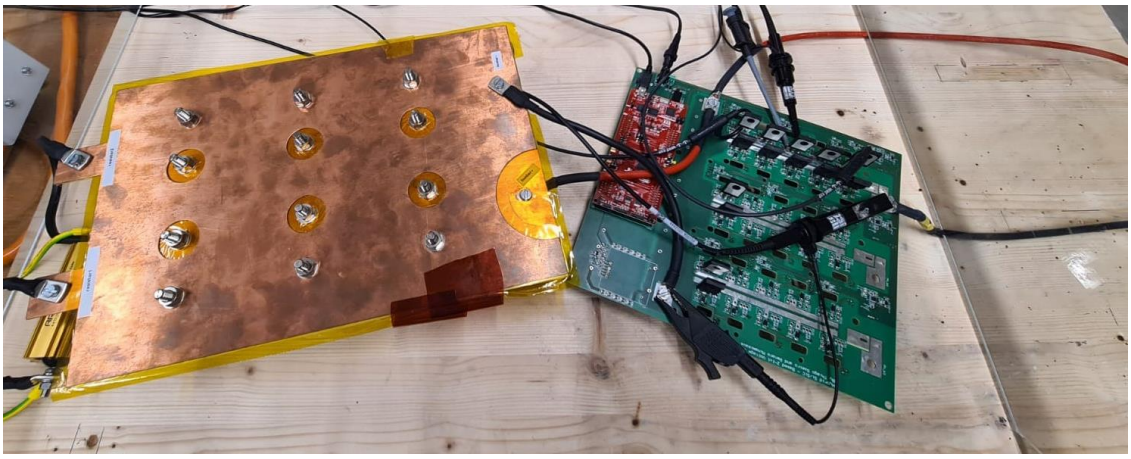

Figure 8. Picture of the XS-cross hybrid double pulse tester (for test of co-packs)

Figure 9 displays the switching waveforms for a XS-hybrid switch featuring SiC MOSFETs and Si co-pack IGBTs, showing the turn-on and turn-off events.

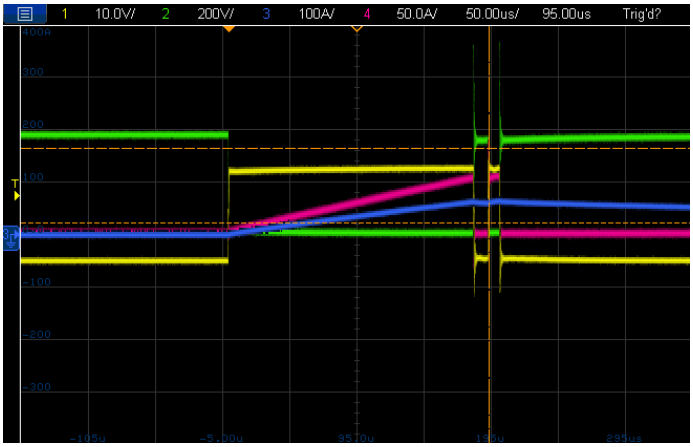

Figure 9. Typical switching waveforms for the XS-cross hybrid switches (yellow- gate source voltage, green- voltage across device, pink- current through device, blue-inductor current)

Figure 10 shows the total switching losses for different ratios of Silicon Carbide to Silicon devices in the hybrid configuration over a wide range of current. The new testing setup also characterized the switching losses for a particular ratio in the gearing mechanism, where in devices in parallel are turned on depending on the value of load current.

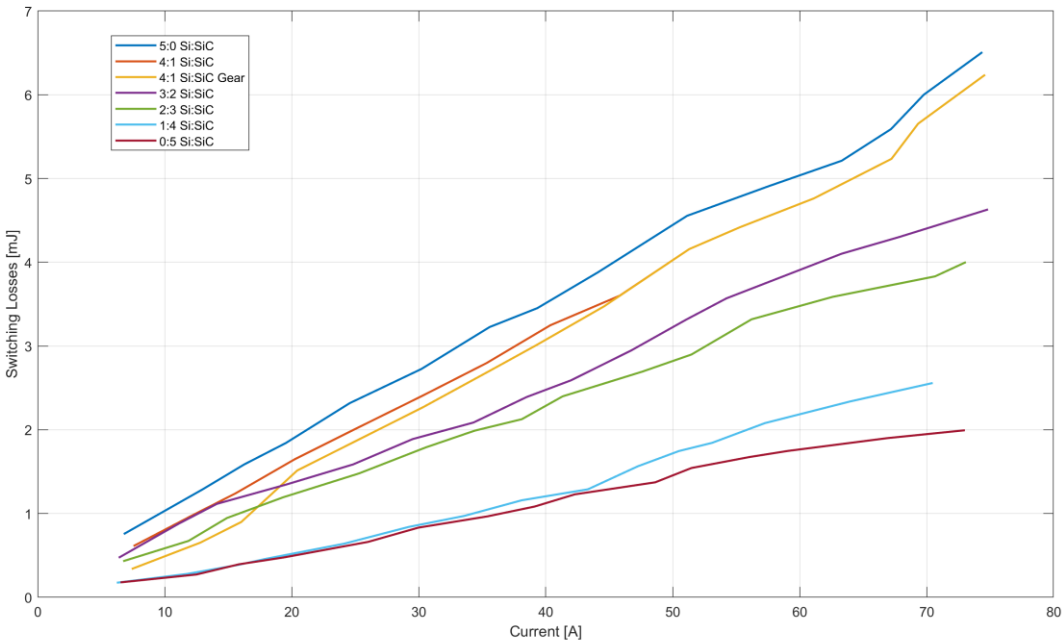

Figure 10. Total switching losses of different combinations of SiC MOSFETs and Si IGBTs

Using the switching losses extracted from the double pulse tester, we have further developed simulation using WLTC drive cycles protocols to assess the potential of the XS-cross hybrid inverter.

3.2 Inverter prototype

Adjustable Hybrid Switch Inverter (AHS)

Switching losses of transistors in different ratio of Si to SiC were estimated using double pulse test and the results helped to determine an optimal ratio of SiC to Si devices namely (1:4). This ratio was selected based on calculation of switching losses and cost in all different configuration possible in a hybrid switch. The proposed ratio of SiC to Si devices, namely 1:4 can be used as the single switching device in a 3-phase inverter system. Thus, the AHS inverter proposed here is depicted in Figure 11. So instead of each switch of a three-phase inverter, there are 1 SiC MOSFET and 4 Si IGBTs.

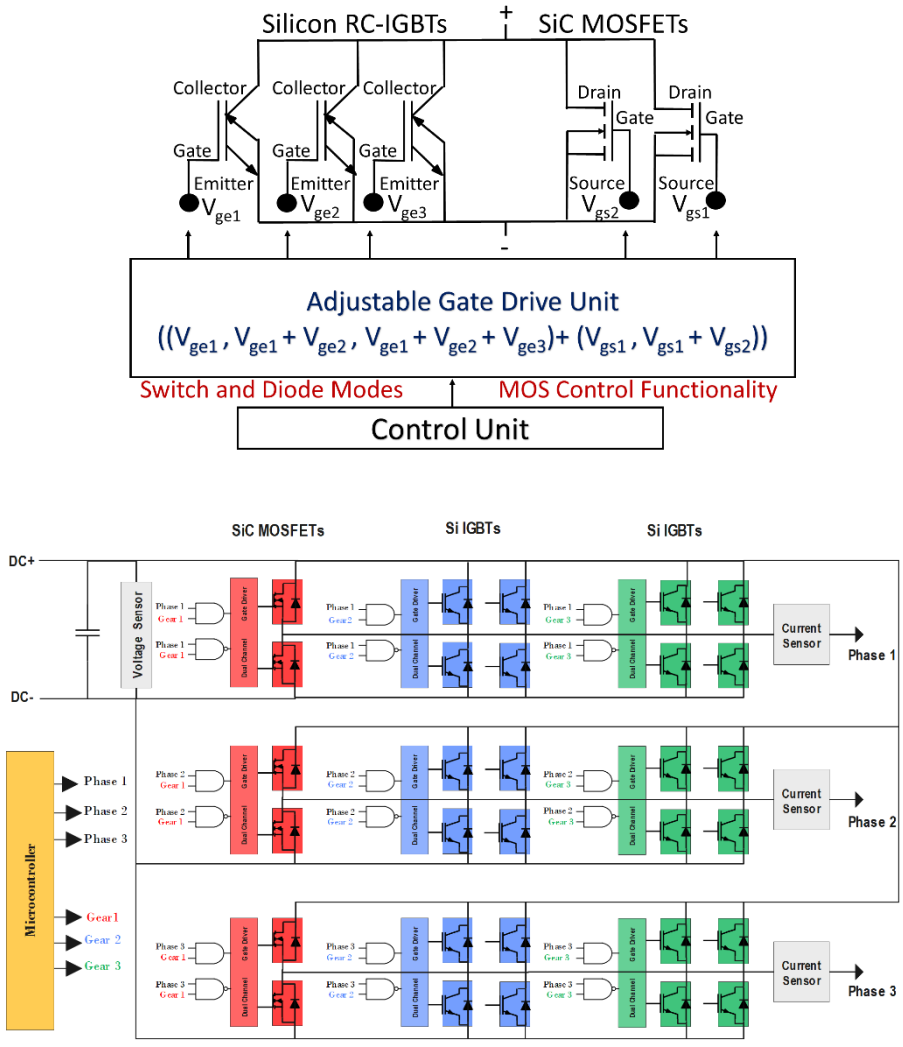

Figure 11. Circuit diagram of three phase AHS inverter

Gearing Mechanism

Although, the SiC MOSFETs offer a very good conduction at lower current and IGBTs offer better conduction at higher currents, the switching losses persist in all the cases. This problem is solved using the gearing mechanism where in all the transistors are not in operation always, and that is the basic concept of the adjustable hybrid switch. The SiC MOSFETs are always on in the inverter circuit, whereas the IGBTs are turned on depending on the load condition. Higher the load, a greater number of IGBTs in parallel are turned on. Thus, in first gear, only SiC MOSFETs come up in the circuit. Under the requirement of higher torque or speed, the gear is shifted to second position wherein 1 or more IGBTs are turned. In the next gear, again a set of IGBTs will be activated and so on. The proposed gearing mechanism will be activated using an intelligent control mechanism optimised for the speed, torque, switching frequency conditions. This system ensures that not all the devices are turned on always and increases the life span of the inverter with improvement in efficiency than Si based inverter and decrement in cost than SiC based inverter. The gear levels and corresponding operating transistor is shown in table 1.

Gear Levels	SiC MOSFET	Si IGBT 1	Si IGBT 2	SI IGBT 3	Si IGBT 4
Gear 1	x				
Gear 2	x	x	x		
Gear 3	x	x	x	x	x

Converter specifications

The rating of a normal inverter for automotive applications varies in the range of 75 kVA (Nissan Leaf) to 200 kVA (Tesla Model S). [2] The kVA ratings are based on the inverter hardware and are greater compared to the kW ratings that are based on the load connected. The design of low power rated inverter can be adopted for higher power by slight modifications in the designs, accessory components and adding additional transistors in parallel across each phase. Due to the limitation in the laboratory, the inverter developed here is downrated for lower power, but with the same ratio of SiC to Si devices.

The maximum DC-link voltage for an E-car is currently around 400 V. [2] The designs of hybrid inverter developed here are adapted for a voltage of 380 V as in conventional inverters. With a ratio of 1:4 of SiC to Si, the minimum number of transistors that can be implemented in the inverter is 5. As the power is downrated, the transistor rated for 15 A or 20A is chosen and can contribute to a peak current of 75 A per phase. The power can be increased by choosing higher current rated devices or by adding more transistor in parallel that obeys the 1:4 ratio or by both methods.

The summary of the ratings of the XS- cross hybrid inverter is listed in the Table 2.

Name	SHINE Hybrid Inverter
Maximal DC Voltage	380 V
DC Current	63 A
Maximum line to line voltage	232.56 V
Continuous output Current	62A
Power Rating	24 kW
Switching Frequency	10 kHz

Table 2. Rating of SHINE Inverter

Voltage Source Inverter Design

The following individual components are designed and produced:

Power Semiconductor Transistors:
Power semiconductor transistors are the main components in the converter and are responsible for switching the voltages on and off. Power transistors are available in different forms in market, namely the discrete devices and the power modules. Different inverter manufacturers implement the hardware with both discrete and modules. To implement the hybrid inverter with gearing mechanism, a ratio of 1:4 SiC to Si devices are recommended and such packages are not available as modules. 1.2 kV, 15 A rated discrete IGBT devices and 1.2 kV, 20A rated discrete SiC MOSFETs in TO-247 packages are used here to develop the XS Cross Hybrid inverter. The SiC MOSFET is chosen from Cree, namely the C2M0080120D and the Si IGBTs from Infineon, namely IKW15N120CS7. [3] [4]

Gate Drivers:
The transistors are turned on and off by applying PWM pulses across the gate and source terminals in SiC MOSFET and across gate and emitter terminals in Si IGBT. The gate drivers hereby charge and discharge the gate capacitances to switch the transistors. The gears are controlled through the gate drivers and hence those devices in separate gears are driven by separate gate drivers. Gate drivers must be different for devices that are in different phases. Thus, the number of gate drivers required for a geared hybrid inverter depends on the phase in which the transistor is and the number of gear levels. The hardware developed here therefore requires a total of nine 2 channel gate drivers for the planned topology. In house gate drivers incorporated with short circuit clamping, under voltage protection, active miller clamping, and desaturation protection are developed. The high- and low-level voltages of the gate drivers are +12V/-5V.

DC- Link:
DC link filter consisting of capacitor serves to limit the voltage fluctuation at the inverter input terminals and ensures that the fluctuating component of the dc link current is reduced within a low specified

acceptable level.[5] The bus link capacitor is used in DC to AC inverters to decouple the effects of the inductance from the DC voltage source to the power bridge. Six capacitors rated 100uF and 500V are connected in series and parallel combination on the main PCB to form a planar structure to reduce parasitic inductance.

Thermal management system:
The loss across the device is mostly dissipated in the form of heat and is taken away using an active water-cooled thermal system to ensure that the junction temperature do exceed the limits. The devices are cooled by spreading the heat at the junction in a more efficient way to the outside ambient temperature through heat sinks, thermal insulations, and the casings. Three aluminium heat sinks are used for all three phase and a single sink can hold all the ten transistors of each phase. Thermal insulating pads created the insulation between the transistors case and the heat sink. Thermal paste also adds to thermal conductivity. [6]

Sensors:
A high voltage DC sensor from LEM (DVC 1000P) [7] is used to measure the input voltage of the three-phase inverter. Three hall effect current sensors (Allegro ACS Series) are connected at the output of the inverter in series to each phase to measure the load current. Both the sensors give secondary outputs and are perfectly isolated from primary circuit. The secondary outputs are less than 5V and can be directly connected to the analog inputs of the controller.

Controller:
The Texas Instrument TMS320F28379D controller is the brain of the inverter system that decides the level of the operation of the gear level. This decision is based on the feedback received from the sensors connected in the circuit. In addition, it is the main component that produces the PWM pulses which are then fed to the input of gate driver boards for amplification. A simple feedback loop from the circuit sensors to the controller decides the amplitude and frequency of the sine wave fed to the PWM modules integrated in the controller. The controller is programmed in MATLAB to produce the sine wave at a switching frequency of 10 kHz. These modules generate the PWM pulses and controller feeds it to that gate driver operating in a particular gear level. [8]

Power PCB:
PCBs in power electronics are most importantly designed to minimize wire lengths and thus reduce stray inductance and EMI efficiently. The main PCB here holds all the transistors, DC link capacitors, voltage and current sensors, controller, circuits for gear mechanism and ports to connect the gate drivers.

The summary of the different main blocks of the inverter is shown in Figure 12.

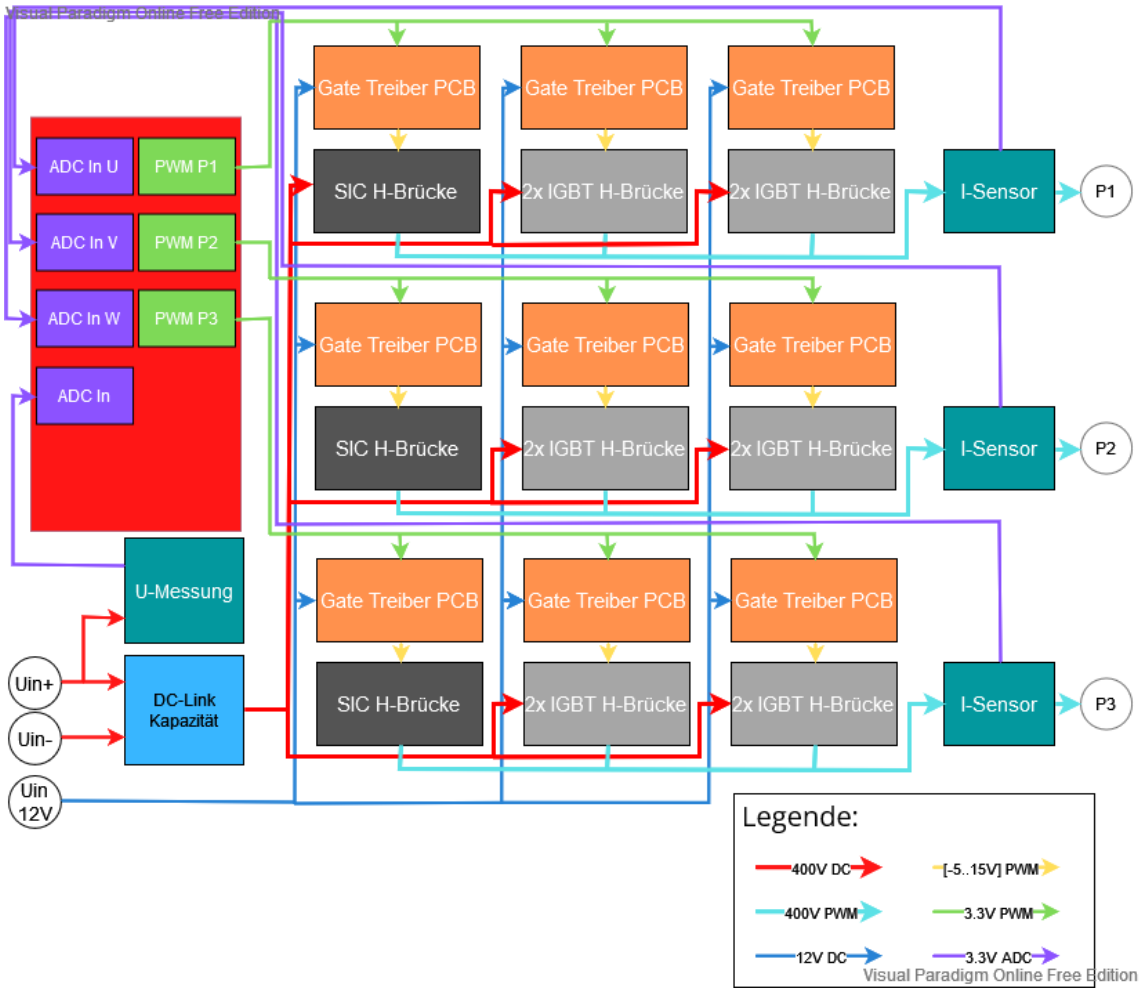

Figure 12. Block diagram of the prototype

Assembly:

The components designed as in the previous section were ordered or send for fabrication. The controller was programmed and checked for its efficiency. The components were soldered onto the main PCB and individual gate driver boards were subjected to test for its operation. After the successful check, the transistors were fixed onto the heat sink and soldered to the main PCB. Cooling circulation was effectively tested using chillers. Sensors were checked individually with connection to the controller. Preprogramed controller and gate drivers were plugged into the respective sockets on the main PCB. Fully developed prototype was inserted into a plastic case. The final hardware of the XS-Hybrid geared three phase inverter is shown in Figures 13-16.

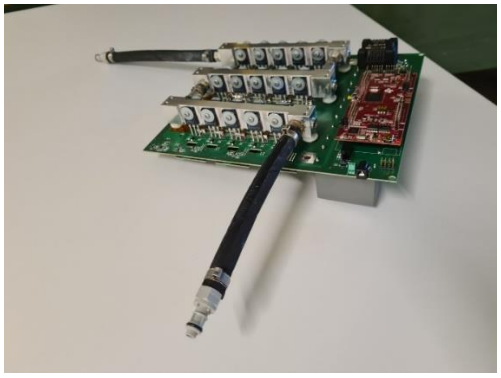

Figure 13. Downside of prototype

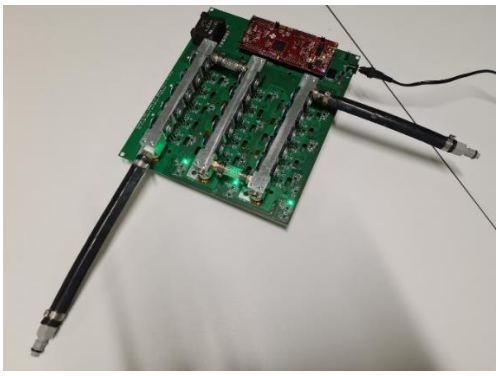

Figure 14. Downside of prototype

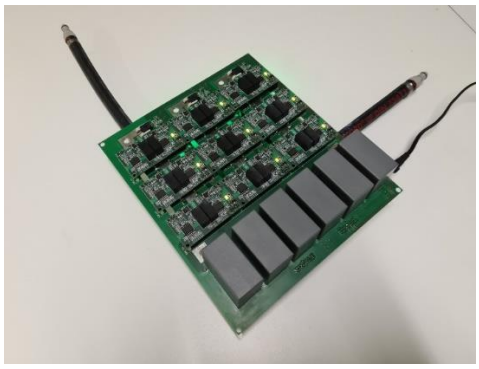

Figure 15. Upside of prototype

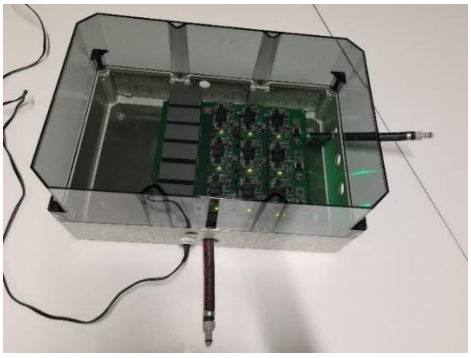

Figure 16. Final prototype in case

Test bench

The DC link capacitors are charged after the operation of the inverter and are subjected to discharge through resistors. Relays are incorporated in the discharge circuit for a better control of turning on and off. The whole system is inserted into plexiglass protection system with locks for the safety of person dealing with the experiment. The hardware inside the protection and safety system is shown in Figure 17.

Figure 17. Converter hardware Inside Protection Cage

The purpose of the test of the inverter is to determine the efficiency of the hardware under different load conditions. The load in the real-life application is a motor and the power source are the batteries. In the laboratory environment, instead of the battery and motor load, a DC power source rated for 25 kW (400 V and 62.5 A) and RL load is used. Varying the resistance in the RL load can change the current through the inverter. [9] Chillers are used to circulate water through the heat sinks. The whole experimental setup is shown in Figure 18.

Figure 18. Experimental Setup

To extract the efficiency of the inverter system, a power analyser is used. Current sensors are clamped onto the three phases of the output of the inverter and voltages connected between the phase and the neutral point. The input values are read from the power source and all output sensors are connected to the power analyser. This device records all the measurements and calculates the single power in each phase and the total power. The Figure 19 depicts the measurement of the inverter parameters using the power analyser and its recording on to the laptop via software.

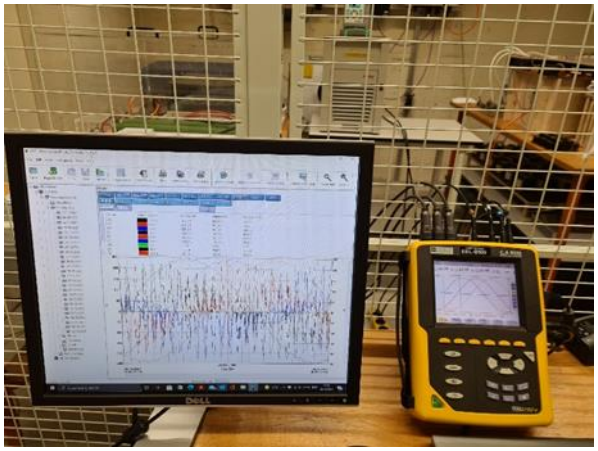

Figure 19. Power Analyser setup

This characterization of the inverter was followed by setting up an EV drivetrain as shown in Figures 20 and 21. The platform included a 30 kW permanent magnet synchronous motor (6500 rpm and 40Nm, EMRAX 188) and two of the 10 kW k10 eddy current brakes (6000 rpm, 27 Nm). The controller of the inverter is loaded with a closed loop field-oriented control program and receives signal from the hall sensor of the motor. The controller then adjusts the PWM pulses using space vector modulation to control the speed of the motor.
The eddy current brakes come with power supplies which can be regulated to change the input current to the brakes. The brakes torque is controlled using DAQs, power supplies and load cells and has specific software to accomplish this task.

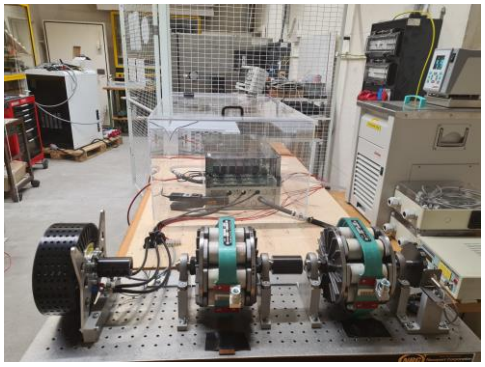

Figure 20. EV Drivetrain

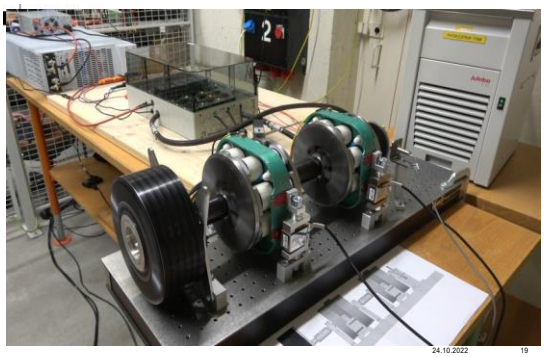

Figure 21. Inverter in test in the EV drivetrain

Inverter characterization

It is also possible to connect voltage probes across any points and ground terminals to observe waveforms on oscilloscope. The PWM pulses were measured across the gate and source terminal of MOSFET and gate and emitter terminal of IGBT. The output of the gate drivers applied to the transistors in each phase is shown in Figure 22.

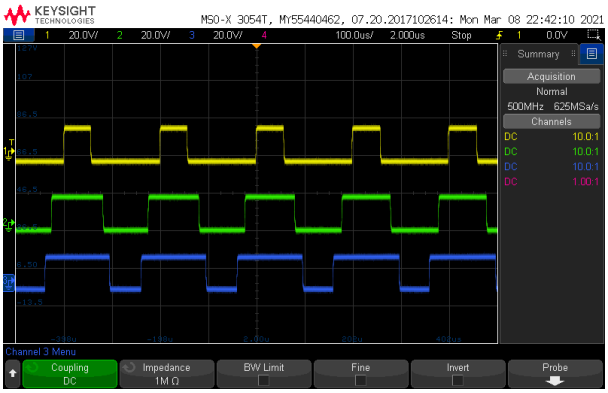

Figure 22. Gate driver PWM pulses

Figure 23 shows the result of the no load test of the inverter at 380V. In this test, no load was connected across output of the inverter and therefore no current was passed through the inverter. The three probes were connected between phases.

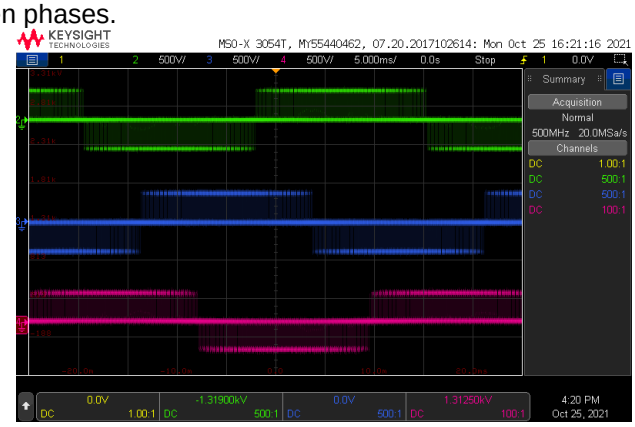

Figure 23. Phase to phase voltages

Figure 24 depicts the screenshot of oscilloscope when the inverter was subjected to load test at 380V and RL-Load. The three phase sinusoidal waveforms can be clearly observed at the output of the current sensors connected in each phase.

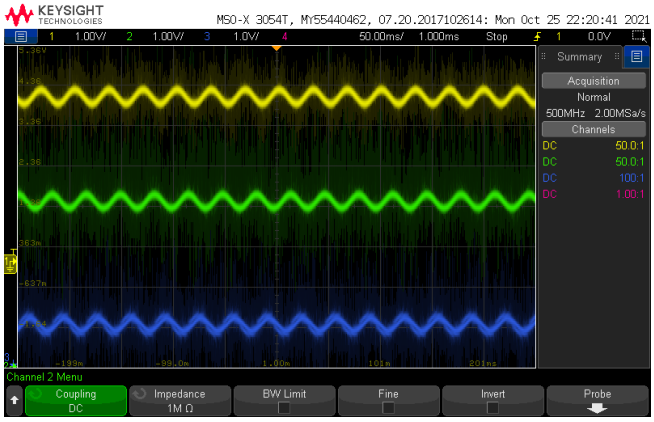

Figure 24. Three phase load current

Figure 25 shows the recorded measurement from the power analyser under load test. It is to be noted that the third phase current is inverted, and the sensor was connected in reverse direction for a better illustration.

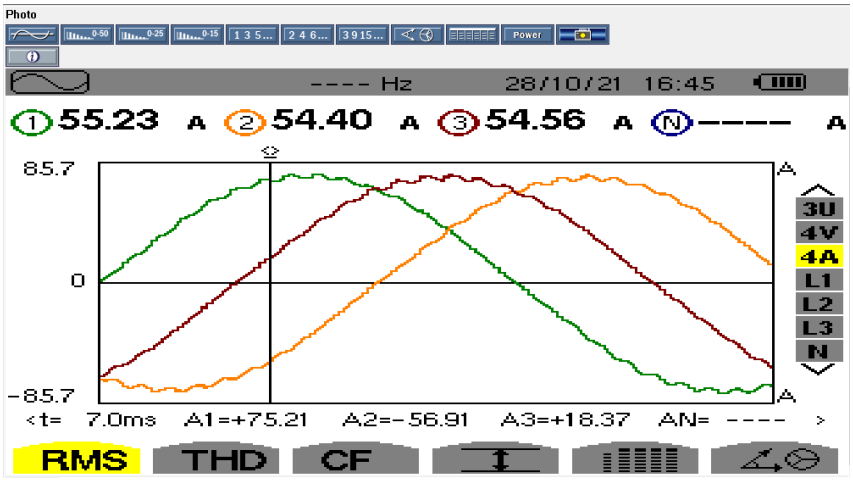

Figure 25. Three phase load current as observed on power anaylser

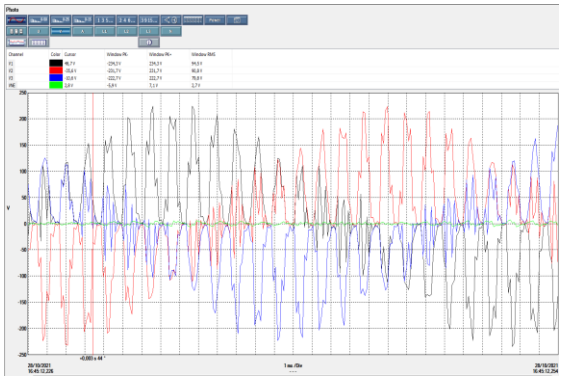

Figure 26. Three Phase Voltage

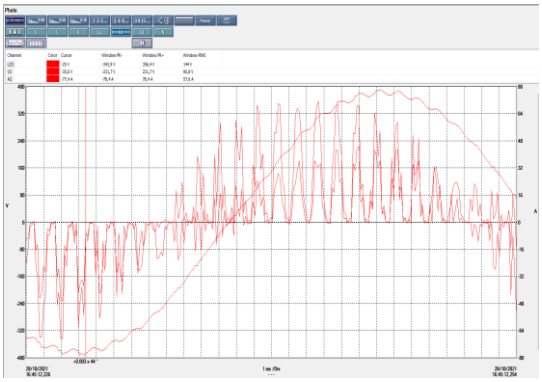

Figure 27. Single phase voltage and current

Figure 26 illustrates three phase voltages. Figure 27 shows the single-phase parameters (current and voltage). These are the depictions from the power analyser when the inverter was subjected to load test.

The load test was conducted on the developed hardware at 380V and varying current flow through the inverter. This was achieved by varying the resistance in the RL load. For each of the load condition, input voltage and current were recorded from the power source panel and multiplied to obtain the input power. The total output power was recorded from the measurements of the power analyser in each case. The ratio of the output to input power gives the efficiency of the VSI hardware. The obtained data was processed and plotted for efficiency versus normalised output power in MATLAB. The experiment was repeated for non-geared hybrid configuration for the comparison to the geared hybrid inverter. The efficiency of full IGBT and full SiC inverter in the same rating and same semiconductors are estimated in PLECS software. *The PLECS simulations are calibrated to the thermal and electrical properties of the*

real hardware. This ensured the inclusion of any stray parameters into the simulations from the experimental setup.

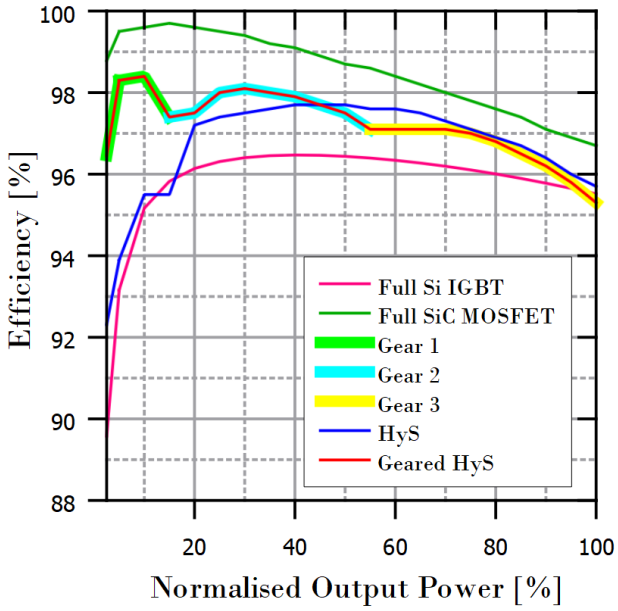

Figure 28. Efficiency Curve

Figure 28 shows and compares the efficiency of the full Si IGBT, geared HyS, non-geared HyS and full SiC MOSFET inverters for the full range of power The best efficiency as expected is for the SiC MOSFET inverter. The full Si IGBTs based converter exhibit the least efficiency in the low load region. The non-geared hybrid configuration with 1:4 ratio of SiC MOSFET to Si IGBT showed a better performance as illustrated. Although no gears are implemented into this configuration, the difference in resistance of both devices leads to unequal current sharing and forces IGBTs not to conduct majorly up to 15% load. This accounts to the roughness in the efficiency curve at 15% load. However, the switching losses of the turned on IGBTs are predominant in this region and reduces the efficiency of the whole system. The point of interest is the geared hybrid configuration wherein the efficiency is considerably improved as comparable to SiC MOSFET in low load region. The shift in gear levels is the reason for the dip in the efficiency after 20% and 60% power points.

The efficiency curves are further investigated to define the losses and improvement in efficiency over the whole driving profile (as shown in Figure 29). WLTP driving cycles are considered for analysis here. The peak efficiency might be better for a particular configuration, however, the total losses over the whole application range is of primary interest.

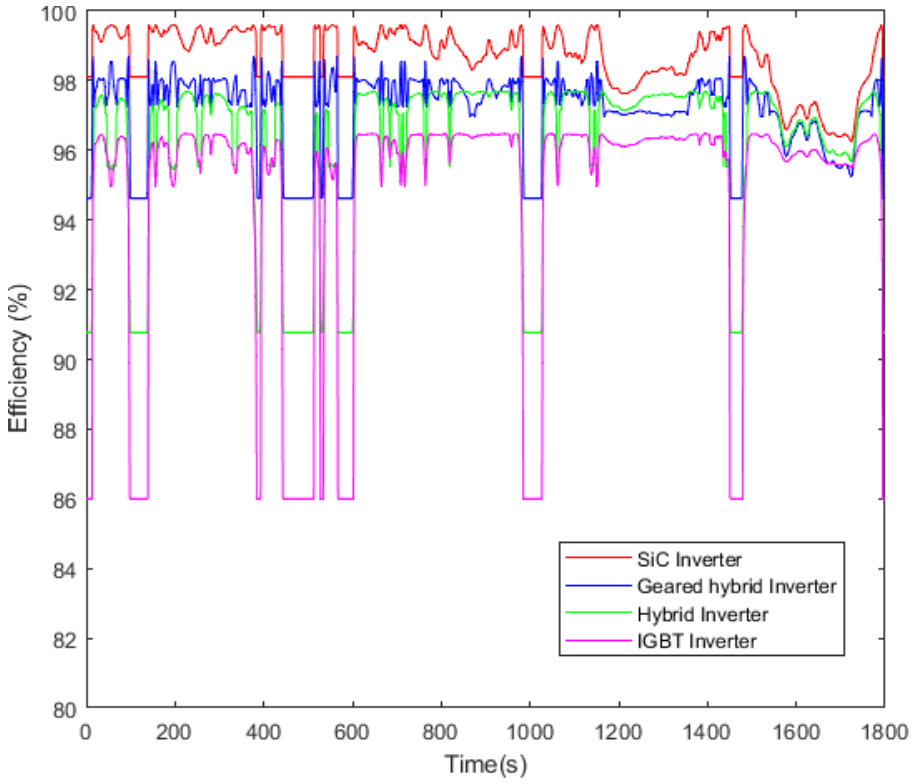

Figure 29. Efficiency Curve over the WLTP driving cycle

The test of the inverter in the EV powertrain showed the compatibility of the inverter with a real EV motor that can be loaded and hence proved the validity of the three-phase geared hybrid inverter in EV application. The working of the system is shown in a separate video. Figure 30 shows the motor tracking the reference speed given as input to the controller and its behavior on increasing the torque using the brakes at the 50th second.

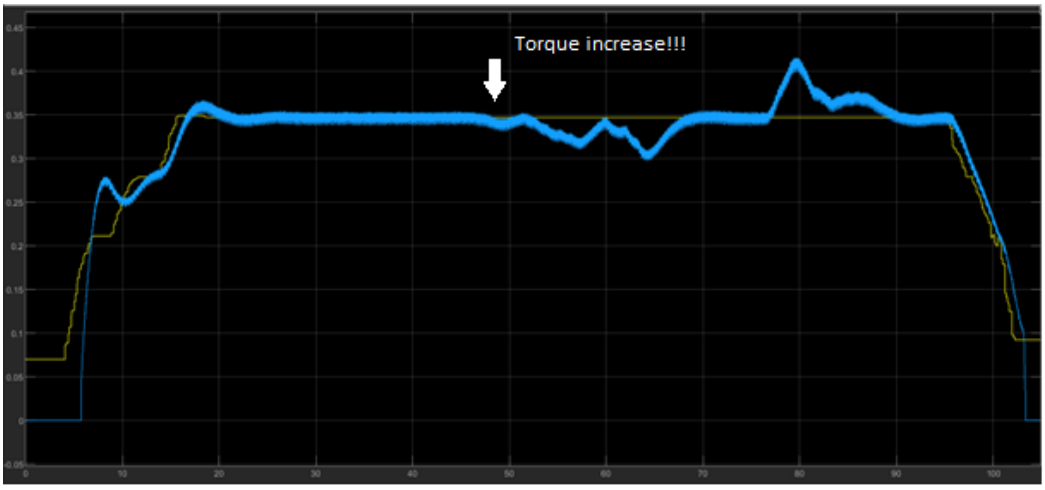

Figure 30. Reference speed tracking of the EV motor

The test results of efficiency test over the driving cycle are summarized in Table 3. Over the full range of the WLTP driving cycle, IGBT inverters are the worst and SiC inverters the best. Hybrid inverters show intermediate performance and geared hybrid inverters exhibit a considerable improvement in efficiency as close as SiC Inverter. This achievement in efficiency without increment in the cost is a successful achievement of this project.

Inverter type	Efficiency [%]
Geared Hybrid (1 SiC:4 Si)	97.09
Non-geared Hybrid (1 SiC:4 Si)	96.1
Full IGBT	94.6
Full SiC	98.64

Table 3. Efficiency Comparison over WLTP driving cycle

3.3 Simulation results

Modular reconfigurable simulation platform

A simulation platform has been developed to test efficiency of the full converter across various driving profiles and car models. The platform is modular and reconfigurable to model different car classes operating under different mission profiles and is composed by three main modules, (see Figure 31):

Mission profile module: for a given car class and driving cycle, this module computes the car mission profile in terms of shaft torque and speed required at every stretch of the given path. The mechanical quantities are then translated in required electrical quantities (voltage and current for a given motor model).

Power train module: simulate the power train including: DC link, power converter, machine and torque load and is parameterized to consider different power range, motor types (IM, PMSM) and converters (Si-, SiC-, Hybrid-based). This simulation will be the base for the diagnostics and prognostics algorithms developed in the following project phase.

Power losses module: For the given mission profile computed by the mission profile module, the power losses module computes the converter conduction and switching losses for the different converters based on Si, SiC and hybrid.

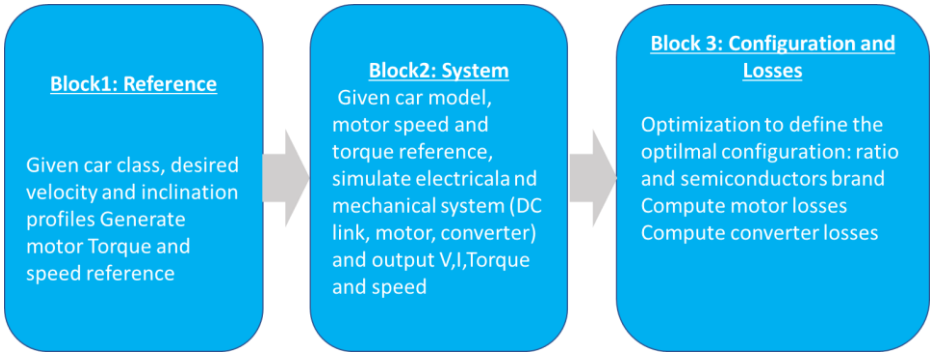

Figure 31. Block diagram of the modular simulation platform encompassing three main blocks

Mission profile module

Based on different car classes and drive cycles characteristics, this module computes what is the car mission profile in terms of shaft torque and speed across the complete path.

Car Classes: Different car classes were considered (see Table 4) and for each class one model was chosen as case study and its parameter were stored to configure the simulation model (see Table 5).

Euro Car Segment	Euro NCAP Class	Examples	Implemented
A-segment mini	Supermini	Citroën C1, Fiat 500, Kia Picanto, Peugeot 108, Renault Twingo	Aston_Martin_Cygnet
B-segment small		Ford Fiesta, Kia Rio, Opel Corsa, Peugeot 208, Volkswagen Polo	Aston_Martin_Cygnet
C-segment medium	Small family car	Honda Civic, Hyundai Elantra, Ford Focus, Toyota Corolla, Volkswagen Golf	Honda_Civic_10._Generation
		Acura ILX, Audi A3, BMW 1 Series, Lexus CT, Mercedes-Benz A-Class	
D-segment large	Large family car	Ford Mondeo, Opel Insignia, Peugeot 508, Mazda6, Volkswagen Passat	Toyota_Prius
		Alfa Romeo Giulia, Audi A4, BMW 3 Series, Lexus ES, Mercedes-Benz C-Class	
E-segment executive cars	Executive	Chevrolet Impala, Chrysler 300, Ford Taurus, Renault Samsung, SM7, Toyota Avalon	BMW_G30
		Audi A6, BMW 5 Series, Cadillac CTS, Mercedes-Benz E-Class, Tesla Model S	
F-segment luxury cars	—	Audi A8, BMW 7 Series, Jaguar XJ, Mercedes-Benz S-Class, Porsche Panamera	BMW_G30
S-segment sports coupés	—	Bugatti Veyron, LaFerrari, Lamborghini Aventador, Pagani Zonda, Porsche 918 Spyder	
	—	Chevrolet Camaro, Mercedes CLK, Volvo C70, Volkswagen Eos, Opel Cascada	Chevrolet_Camaro_(2015)
	Roadster sports	BMW Z4, Lotus Elise, Mazda MX-5, Porsche Boxster, Mercedes-Benz SLK	

Table 4: Car segments and examples considered in the simulation module mission profile

Classes	Mass [Kg]	Motor max speed [min^-1]	Max speed [Km/h]	Power [KW]
classAB	1000	16000	160	72
classC	1300	16000	170	88
classD	1500	16000	180	108
classEF	1800	16000	210	185
classS	1750	18000	290	485

Table 5: Car characteristics for each segment

Driving Cycle: Different standard driving cycles have been considered composed by basic cycles: city, exurban, exurban and autobahn, autobahn, racing.

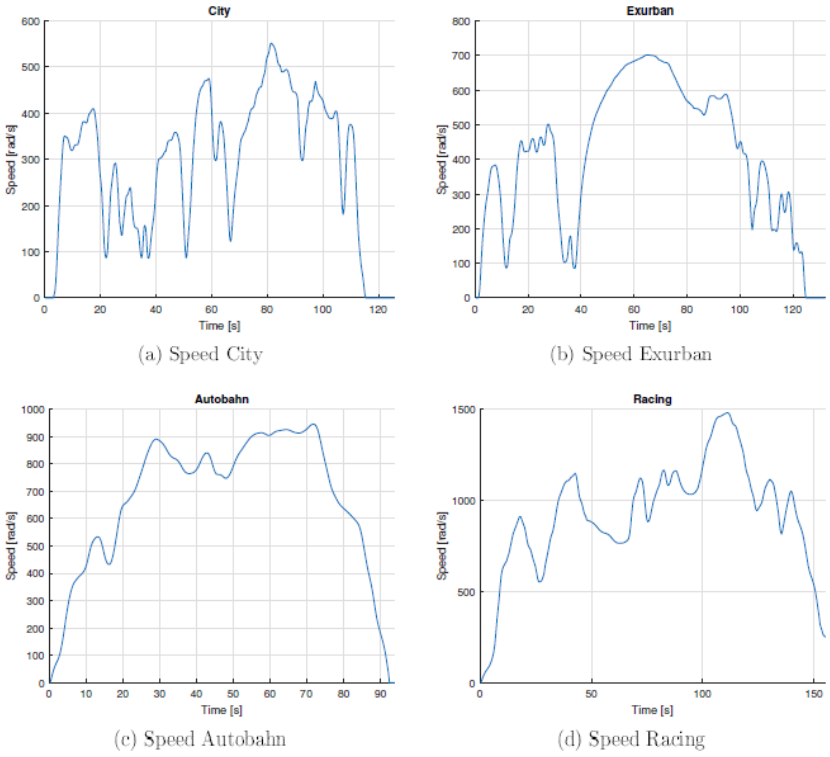

Figure 32: Drive cycles for City, Exurban, Autobahn and Racing

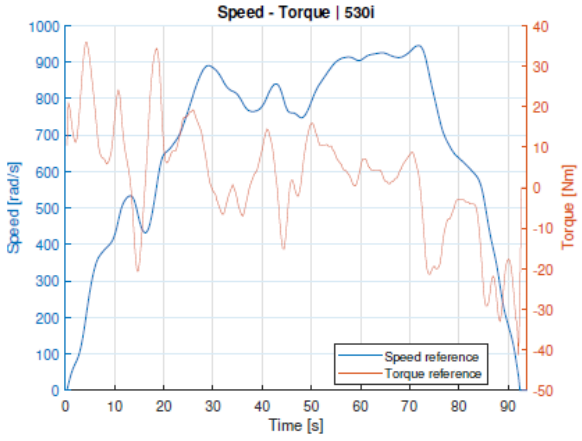

Figure 33: Reference speed and the reference torque for a BMW 530i driving on the autobahn.

For each car class, based on the car physical characteristics and driving cycles, the mission profile was computed.
The four different speed profiles for the vehicle class AB are shown in (a) to (d) in Figure 32. The driving profiles represent approximately the curve which is created during a corresponding journey. Figure 33 shows the reference speed and the reference torque for a BMW 530i driving on the autobahn.

Power train module

The entire physical system consisting of a battery, inverter, motor and thermal model has been implemented in PLECS. The main circuit of the PLECS model is shown in Figure 34. The individual semiconductors are modeled into subsystems with the gate-driver signal as input and the measured values of junction temperature, current, voltage and losses of the semiconductors as output. Four different configurations of the semiconductors were considered: full IGBT, full MOSFET, Hybrid (IGBT and MOSFET) ratio once 1:1 and Hybrid-Switched (IGBT or MOSFET).

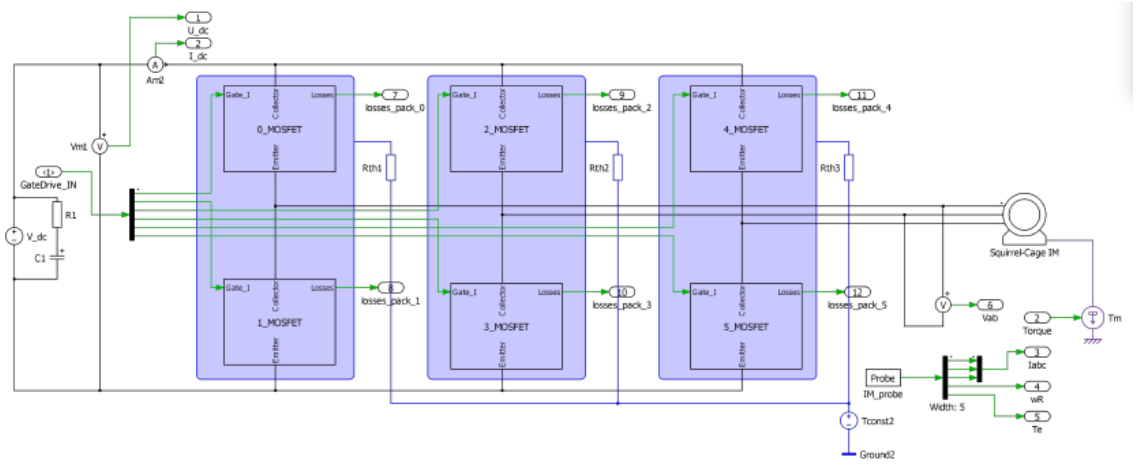

Figure 34: Power Train Model in PLECS

Power losses module

The thermal system in PLECS is used to compute the losses of the individual components. The values for thermal capacitance and thermal resistance were taken from the datasheets of the respective semiconductors. The losses are also coded in a Matlab file using the formulas below:

Conduction Losses

$$P_{condigbt} = I_{rmswigbt}^2 * R_{ceigbt} + I_{avigbt} * U_{ce0igbt}$$
$$P_{conddiode} = I_{rmswiode}^2 * R_{ceiode} + I_{aviiode} * U_{pn0diode}$$
$$P_{condsic} = I_{rmssic}^2 * R_{dssic}$$

Switching Losses

$$P_{swigbt} = f_{mot} * \frac{U_{dc}}{U_{hyb_{test}}} * (a_{xy_{igbt}} * I_{sic}(t)^2 + b_{xy_{igbt}} * I_{sic}(t) + C_{xy_{igbt}}$$
$$P_{swdiode} = f_{mot} * \frac{U_{dc}}{U_{hyb_{test}}} * (a_{xy_{diode}} * I_{sic}(t)^2 + b_{xy_{diode}} * I_{sic}(t) + C_{xy_{diode}}$$
$$P_{swsic} = f_{mot} * \frac{U_{dc}}{U_{hyb_{test}}} * (a_{xy_{sic}} * I_{sic}(t)^2 + b_{xy_{sic}} * I_{sic}(t) + C_{xy_{sic}}$$

Total Losses

$$P_{igbt} = P_{condigbt} + P_{swigbt}$$
$$P_{diode} = P_{conddiode} + P_{swdiode}$$
$$P_{sic} = P_{condsic} + P_{swsic}$$

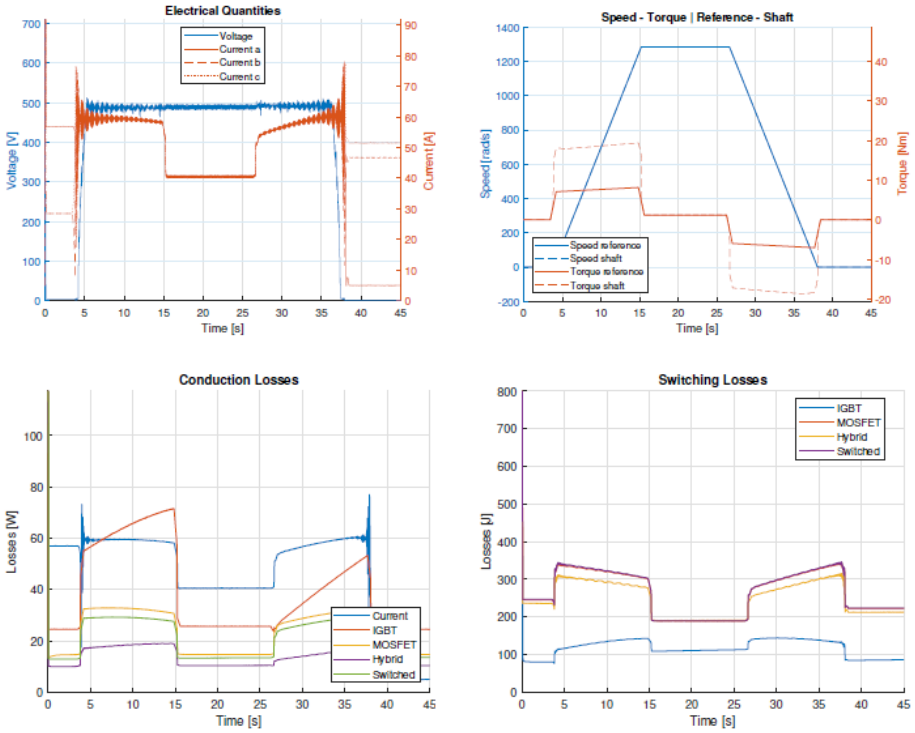

Figure 35: Speed reference and torque load for a trapezoidal driving profiles. Associated current and voltage profiles and losses for a car class AB with the different configurations: IGBT, MOSFET, Hybrid and Switched

The combined result of all the subblock allows to compute the complete losses profile for specific driving cycles and car classes, see Figure 35.

3.4 Summary Results Layout and e-gear design

Converter Efficiency-Cost analysis and configuration selection

To select a suitable hybrid configuration for each car class, an efficiency-cost analysis has been performed for each hybrid configuration, considering *different Si/SiC ratios and device brands*, for each car class. First the efficiency of the different hybrid converters has been evaluated considering switching and conducting losses over a range of power, an efficiency-cost score has been defined to rate each configuration based on efficiency and price.

Efficiency

To evaluate the converter efficiency, the switching and conduction losses of different semiconductor combinations has been computed and compared.

For the analysis the following combinations were tested:

- Si-IGBT only
- SiC-MOSFET only
- SiC-MOSFET / Si-IGBT hybrid in 1:1 ratio
- SiC-MOSFET / Si-IGBT hybrid in 1:4 ratio

Efficiency curves were generated using the IKW40N120CS6 from Infineon and C2M0040120D from Cree. The Simulation parameters used can be looked at in table 6.

DC-Link voltage	400V
T_{amb}	75°C
R_{th} (Heatsink to Ambient)	0.03 K/W
f_{inv}	10kHz
f_{out}	50Hz
U_{out}	240V

Table 6 Simulation Parameters simple case

To guarantee the same total number of semiconductors in every configuration, the distribution of semiconductors described in Table 7 was used.

Configuration	No of IGBTs	No of SiC
Only IGBT	10	0
Only SiC	0	10
Ratio one SiC to one IGBT	5	5
Ratio one SiC to four IGBTs	8	2

Table 7 Number of semiconductors

As expected, the MOSFET had the best efficiency and the IGBT the worst. The hybrid configurations are located between the two, seen in Figure 36.

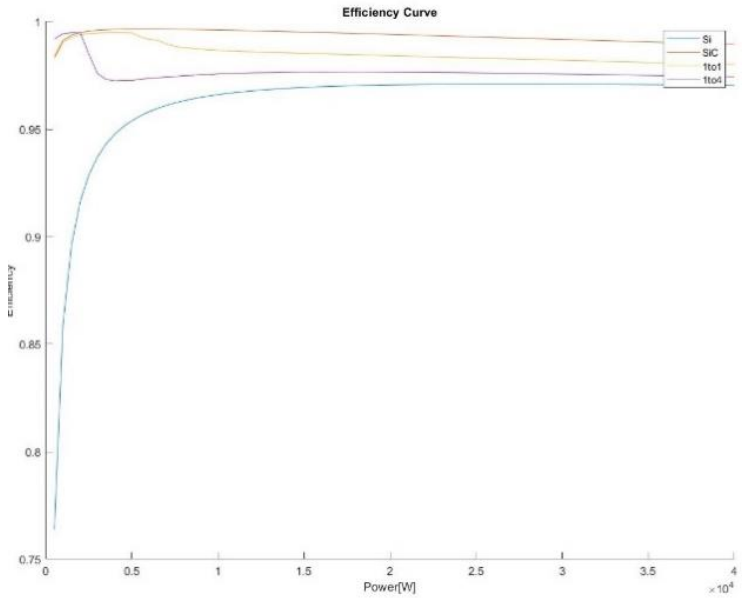

Figure 36 Efficiency-Power Curve Simple Case: violet curve 1 to 1 ration of Si and SiC, violet curve 1 to 4 ratio SiC-Si

The Semiconductors used for this task can be seen in Table 8.

Name	Part number
Discrete SiC	
cree 60A Die	C2M0080120D
cree 60A	C2M0040120D
Discrete Si	
Infineon IGBT	IKW40N120CS6
Infineon RC IGBT	IHW40N120R3
Module Si	
Fuji IGBT 600A	2MBI600XNG120-50
Fuji RC IGBT 1000A	2MBI1000XRNE120-50
Infineon IGBT4 600A	FF600R12ME4A_B11
Infineon IGBT7 900A	FF900R12ME7_B11
Module SiC	
Infineon SIC MOSFET 500A	FF2MR12KM1P
Rhom SiC MOSFET 200A	BSM180D12P2E002
Rhom SiC MOSFET 300A	BSM300D12P3E005
Rhom SiC MOSFET 600A	BSM600D12P3G001
Wolfspeed SiC MOSFET 400A	WAB400M12BM3

Table 8 Semiconductor models

Different semiconductors combinations have been considered within the compatible modules. Totally, 61 combinations are possible considering the four different inverter types. They have been tested with configurations capable to deliver 72, 88, 108, 185 and 485 kilowatts of power, and pick efficiency has been used for the computation of the CES.

The number of semiconductors was calculated using the following equations.

$$n_{Semis} = \frac{I_{max} \cdot U_{out}}{P_{max}}$$
$$n_{tot\_1to1} = \frac{(I_{Si\_max} + I_{SiC\_max}) \cdot U_{out}}{P_{max}}$$
$$n_{Si} = n_{SiC} = \frac{n_{tot\_1to1}}{2}$$
$$n_{tot\_1to4} = \frac{(4 \cdot I_{Si\_max} + I_{SiC\_max}) \cdot U_{out}}{P_{max}}$$
$$n_{SiC} = \frac{n_{tot\_1to4}}{5}$$
$$n_{Si} = n_{SiC} \cdot 4$$

Each simulation was run for different operating points ranging from 1 Watt to the maximum power of 72, 88, 108, 185 and 485 kilowatts. The results of the simulation contained the pick efficiency, number of semiconductors and power for each operating point.

Cost

The cost of each individual semiconductor can be taken from Table 9.

Silicon	CHF
IKW40N120CS6	8.41
IHW40N120R3	7.2
2MBI600XRNE120-50	102.33
2MBI1000XRNE120-50	135.71
FF600R12ME4A_B11	306.13
FF900R12ME7_B11	301.49
C2M0040120D	31.16

Silicon Carbide	CHF
C2M0080120D	15.23
FF2MR12KM1P	949.33
BSM180D12P2E002	612.57
BSM300D12P3E005	1241.83
BSM600D12P3G001	1616.32
WAB400M12BM3	674.99

Table 9 Cost of Semiconductors

Converter Efficiency/Cost score evaluation

In the table the cost of the semiconductors was added, and a cost-efficiency score was calculated using the formula**Fehler! Verweisquelle konnte nicht gefunden werden.**:

$$CES = \frac{Price}{(1-\eta_{\emptyset})}$$

The lower the score, the better the cost-efficiency. The efficiency has an impact on how much heat is produced in the system, the more heat the semiconductors produce, the more capable the cooling system needs to control the temperatures. A better cooling system is more expensive, larger and adds more weight to the vehicle, which are aspects decreasing the range and efficiency and increasing the price of the EV.

Interestingly, the best cost efficiency score was not always the same ratio combination as for the lowest power range it was a 1:4 ratio and for the four others a 1:1, although both ratios perform well for all 5 power ranges.

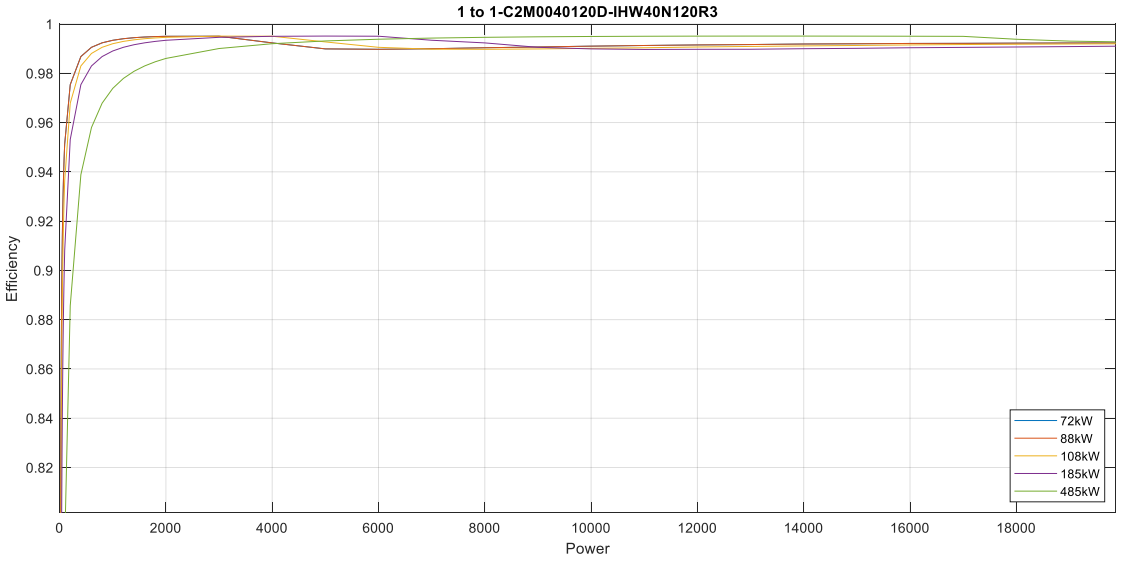

There were four semiconductors, which performed particularly high in the cost-efficiency score. Those

Figure 37 Efficiency of multiple small and two large Semiconductors

were two IGBT models from Infineon (IHW40N120R3 and IKW40N120CS6) and two SiC MOSFET models from Cree (C2M0040120D and C2M0080120D).
The cost for semiconductors is proportional to their power capability. As for the efficiency, for both semiconductor types especially the IGBTs have a higher efficiency at higher power throughput as can be seen in Figure 37. The smaller semiconductors can be connected in parallel to deliver more power which is better adjusted for the power needed.

The cost-efficiency score provides a mean to select the most suitable combination for a car class. The combination with the best cost-efficiency score, the most efficient with a maximum deviation of three times the cost-efficiency score of the one with the best and the cheapest combination with a maximum deviation of three times the of the cost-efficiency score of all five power range are summarized in table 10.

Power range	**Best cost-efficiency score**	Eff. / Price	Most efficient	Eff. / Price	Cheapest	Eff. / Price
72 kW	**1:4 C2M0080120D IHW40N120R3**	98.94% 264.18$	SiC only C2M0080120D	99.35% 731.04$	Si only IHW40N120R3	97.21% 216$
88 kW	**1:1 C2M0080120D IHW40N120R3**	99.18% 538.32$	SiC only C2M0080120D	99.35% 913.80$	Si only IHW40N120R3	96.77% 259.20$
108 kW	**1:1 C2M0080120D IHW40N120R3**	99.16% 672.90$	SiC only C2M0040120D	99.55% 1308.72$	Si only IHW40N120R3	96.34% 302.40$
185 kW	**1:1 C2M0040120D IHW40N120R3**	99.34% 1380.96$	SiC only C2M0040120D	99.65% 2243.52$	1:4 C2M0080120D IHW40N120R3	98.34% 792.54$
485 kW	**1:1 C2M0040120D IHW40N120R3**	99.65% 3682.56$	1:1 C2M0040120D IKW40N120CS6	99.65% 3798.72$	1:4 C2M0080120D IHW40N120R3	98.19% 1849.26$

Table 10 Configuration for best semiconductor selection

The benefits of using a hybrid configuration in an EV inverter, not only are shown in efficiency but also in the price. The losses in hybrid configurations are not far from the losses of a pure MOSFET configuration but the cost is far lower. The use of the hybrid configuration reduce the cost of a pure MOSFET configuration by as much as 63% and only giving up around 0.4% of peak efficiency. Compared to an only IGBT configuration a 1:4 configuration can be between 3-10% more efficient for around 50% more cost. However, this cost only represents the cost for the semiconductors and not the cost for cooling and magnetics, which is less expensive for more efficient inverters. Because the price difference between the best four 1:4 combinations cost and the best four only IGBTs configurations for the highest power range is only between 100 and 250USD it can be assumed that the more expensive cooling solution for the IGBTs can exceed this price range.

The selection of semiconductors depends on a series of factors, which all components are related to. The minimum power range, the minimum and maximum size, the minimum efficiency, the minimum driving range, and maximum price of the vehicle all should be defined before starting to select the components to have set boundaries. There might have to be implemented changes on those boundaries, but the designer has a goal to work with. For the selection of the semiconductors, the price, efficiency, and size of the vehicle are key.

Optimal torque control for e-gear

To implement an automatic gear concept, we designed an optimization based torque controller, that starting from the mission profile and driver selected driving mode, sport or eco, define the optimal torque, and consequently acceleration to track the given reference speed while maximizing the energy efficiency.

We consider the dynamic model of the shaft speed as function of the electrical torque produced by the drive and the torque load of the car

$$\frac{d\omega}{\mathrm{dt}} = \mathrm{K}\,(\tau_e - \tau_l)$$

The torque load τ_l can be assumed to be measured or estimated and compensated for or.

τ_e is the eltrcical torque produced by the drive.
To track a reference speed ω^* the standard PID based torque controller guarantee error free steady state tracking

$$\mathrm{e} = \omega - \omega^*$$
$$\sigma = \int (\omega - \omega^*) dt$$
$$\tau_e = -\mathrm{K}_1 e - \mathrm{K}_2 \sigma$$

It can be shown that the closed loop system with applied the PI controller will guarantee convergence to the reference speed.

$$\frac{d\binom{e}{\sigma}}{\mathrm{dt}} = \begin{pmatrix} -K\mathrm{K}_1 & -\mathrm{K}\mathrm{K}_2 \\ 1 & 0 \end{pmatrix} \binom{e}{\sigma} + \binom{K}{0} \tau_l$$

The gains K_1 and K_2 define the system acceleration, that is how fast the system will converge to the required speed. They represent the degree of freedom for the controllers during the transients and can be designed to maximize efficiency, i.e. minimize switching and conductive losses. Based on the car driving cycle, the time variable gains are designed to produce an optimal instantaneous torque, and consequently current, which will define the optimal instantaneous IGBT and Mosfet ratio, in other words, the optimal electric gear ration.
The optimal gains can be defined by solving the optimization problem below:

$$Min_{k1,k2}(\mathrm{J}_{losses} + \mathrm{J}_{damage} - T)$$
$$\text{s.t. } |\tau| < \mathrm{T}_{max}$$

where J_{losses} is the cost representing the losses, J_{damage} is the damage and the torque T constraints will vary depending on the selected driving mode.
In summary the controller guarantees tracking of the reference shaft speed while maximizing the torque for performance and minimize losses resulting in a maximized efficiency.

4 Conclusions

In this work, we have developed a new power electronics topology featuring parallel Si IGBTs and SiC MOSFETs for electric vehicle applications, the so-called Adjustable Hybrid Switch (AHS). This new concept consists on switching individual power devices based on the load current demand, in what we refer as “electronic gear”.

As such, since IGBTs exhibit conduction losses in low load regime, SiC are first activated when low current is needed. As the IGBTs are off, they do not contribute with switching losses. The IGBTs are then just switched on, when high current load is required. The work presented here and the experimental demonstration proves the validity of the proposed concept. The geared hybrid inverter exhibits high efficiency as comparable as SiC inverter and low cost as Si IGBT inverter. In practice, the optimum AHS configuration from the cost-efficiency trade-off was found to be the ration of 1 SiC MOSFET to 4 Si IGBTs. The simulations show that full SiC inverters exhibit up to 9% efficiency enhancement compared to full Si inverter (depending on the WLTP), at about 2.5 times lowers costs. Remarkably, the AHS demonstrated improvement between 5 and 8% efficiency over a full Si converter consistently, besides an improvement over the “non-geared” XS-hybrid.

The concept of electronic gears is a minimalistic change in the control of the hybrid inverter and can be easily implemented to reduce losses than a non-geared hybrid inverter. The geared concept presented is well suited for any application that involves variable frequent operation of the converter electric vehicles. The results obtained demonstrate the performance of the gear concept in term of energy efficiency and cost optimality and the high potential of XS-hybrid configuration and its adaptive version as a solution to address the challenge of efficient power conversion at reduced cost. This opens to the possibility of enabling economic large-scale introduction of electric vehicle and extends to applications beyond mobility.

In conclusion, AHS solutions demonstrated to be promising alternative to the pure SiC solution to be pursued and extended to applications with high power range variability.

5 Outlook and next steps

The first target outlook of the research is to promote its implementation in industry, which has been successfully transferred to the industrial partner MTAL, which will in turn define a strategy for technology its product development strategy. As a main conclusion from this work, the AHS is likely to profit any variable frequency application. One of the most relevant and promising power electronic application is the photovoltaic, which can profit from the AHS for the following reasons:

1. Financial savings because of energy saving is huge, which will increase because of the forecast of high future electricity prices.
2. Energy saving is massive and benefits all customer segments, i.e., residential, commercial and industrial.
3. SiC implementation in early stage and only about 5 companies offer it at the moment. These results will be presented in the next PECTA report in 2023.
4. Market has high granularity and high competition, with more than 1000 players competing for innovation.
5. Installation margins are small and market is cost sensitive.
6. Footprint size is not an issue.

As a next step, we will be investigating the AHS solution performance for photovoltaic application, particularly in comparing its performance with full-SI and full-SiC converters, and to understand its business case potential.

6 Publications

M. Rahimo et al., "An Advanced Adjustable Switch Hybrid (ASH) Concept for High Power Automotive Converters," PCIM Europe digital days 2021; International Exhibition and Conference for Power Electronics, Intelligent Motion, Renewable Energy and Energy Management, 2021, pp. 1-8.

M. Rahimo et al., " Switched hybrid power converters for automotive and methods for operation and diagnostics ", 2019 EU Patent application under review.

7 References

[1] M. Rahimo et al., "Characterization of a Silicon IGBT and Silicon Carbide MOSFET Cross- Switch Hybrid," in IEEE Transactions on Power Electronics, vol. 30, no. 9, pp. 4638-4642, Sept. 2015

[2] J. Reimers, L. Dorn-Gomba, C. Mak and A. Emadi, "Automotive Traction Inverters: Current Status and Future Trends," in IEEE Transactions on Vehicular Technology, vol. 68, no. 4, pp. 3337-3350, April 2019, doi: 10.1109/TVT.2019.2897899.

[3] Infineon, “Datasheet Resonant Switching Series Reverse Conducting IGBT with monolithic body diode IKW15N120CS7“, 19. September 2019. [Online]. Available: https://www.infineon.com/dgdl/Infineon-IKW15N120CS7-DataSheet-v01_00-EN.pdf?fileId=5546d46278d64ffd0178f97db2b905a6 [accessed on August 2020].

[4] Cree, “Datasheet Silicon Carbide Power MOSFET C2M MOSFET Technology C2M0080120D,” September 2019. [Online]. Available: https://www.wolfspeed.com/media /downloads/167/C2M0080120D.pdf [accessed on August 2020].

[5] M. Salcone and J. Bond, "Selecting film bus link capacitors for high performance inverter applications," 2009 IEEE International Electric Machines and Drives Conference, Miami, FL, 2009, pp. 1692-1699, doi: 10.1109/IEMDC.2009.5075431.

[6] J. Ye, K. Yang, H. Ye and A. Emadi, "A Fast-Electro-Thermal Model of Traction Inverters for Electrified Vehicles," in IEEE Transactions on Power Electronics, vol. 32, no. 5, pp. 3920-3934, May 2017, doi: 10.1109/TPEL.2016.2585526.

[7] LEM, “Datasheet Voltage transducer DVC 1000P “, 28. September 2018. [Online]. https://www.lem.com/sites/default/files/products_datasheets/dvc_1000-p.pdf [accessed on August 2020].

[8] J. M. Peña and E. V. Díaz, "Implementation of V/f scalar control for speed regulation of a three-phase induction motor," 2016 IEEE ANDESCON, Arequipa, 2016, pp. 1-4, doi: 10.1109/ANDESCON.2016.7836196.

[9] Rabiei, Ali. “Energy Efficiency of an Electric Vehicle Propulsion Inverter Using Various Semiconductor Technologies.” (2013).